Knowledge-Driven Variational Methods in Medical Image Processing

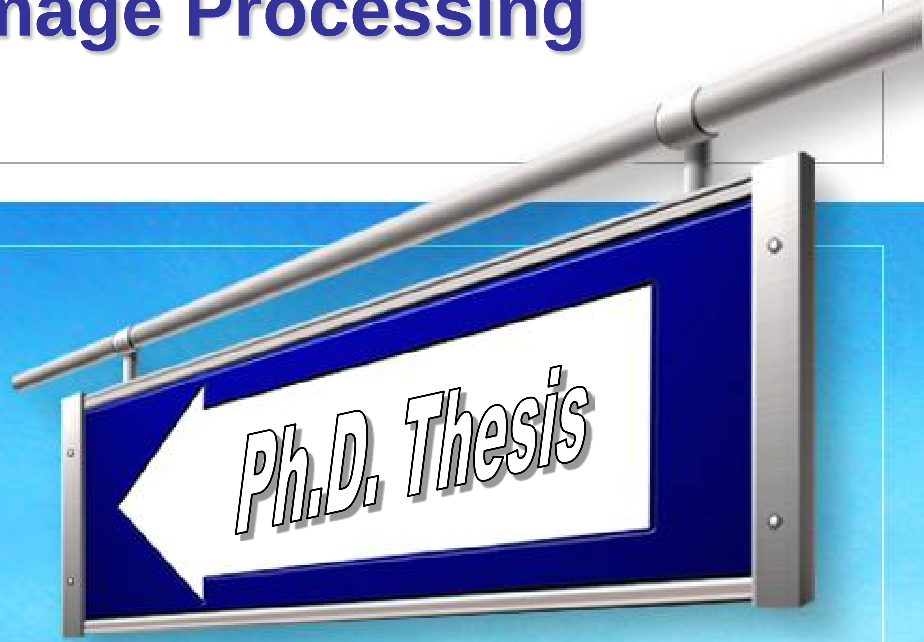

by

Phan Tran Ho Truc

KYUNG HEE UNIVERSITY

December 2008

Department of Computer Engineering

Thesis Supervisor ……………………………………..

Prof. Sungyoung Lee

Department Chair ………………………………………

Prof. Young-Koo Lee

Contents

- Medical Image Processing
- Why Variational Methods?
- Variational Methods in IP
  - Diffusion filtering
  - Active contours
- Knowledge-driven Filtering
  - Hessian-based
  - Directional Filter Bank-based
  - Vessel enhancement
- Knowledge-driven Segmentation
  - Conventional AC models
  - Density distance augmented Chan-Vese AC
  - Bone segmentation
- Contributions and Publications

Medical Image Processing

- Medical procedures make substantial use of image processing.

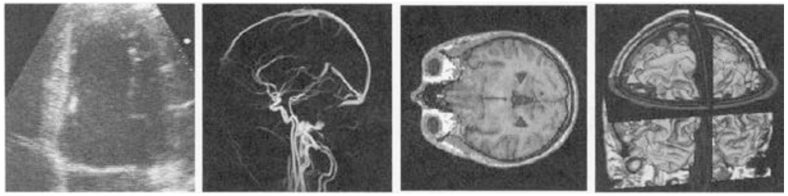

- Medical image processing tasks
  - Enhancement: to bring out obscured details in an image
  - Segmentation: to help measuring medical conditions: vessel size, tumor volume, bone fraction length, …

- Heuristic and low level mathematical operators
  - when and why they work or do not work - unclear
- More sophisticated mathematical tools
  - Variational methods: optimization of cost functions or design of PDEs

Why Variational Methods?

1. Most existing methods can be recast variationally.
2. The theory behind the concept is well established.
   – PDEs are written in continuous setting, making the understanding of physical reality easier → stimulates the intuition to propose new models.
3. Using an energy functional and a descent algorithm, one can easily state when one result is better than another.
4. The use of the calculus of variations allows one to integrate prior knowledge and build quite complicated cost functionals.
   – **Interesting**: knowledge about organs of interest is known a priori.
   – **Necessary: purely image-driven methods** can hardly work for medical images.

Knowledge-Driven

Variational Methods

in

Medical Image Processing

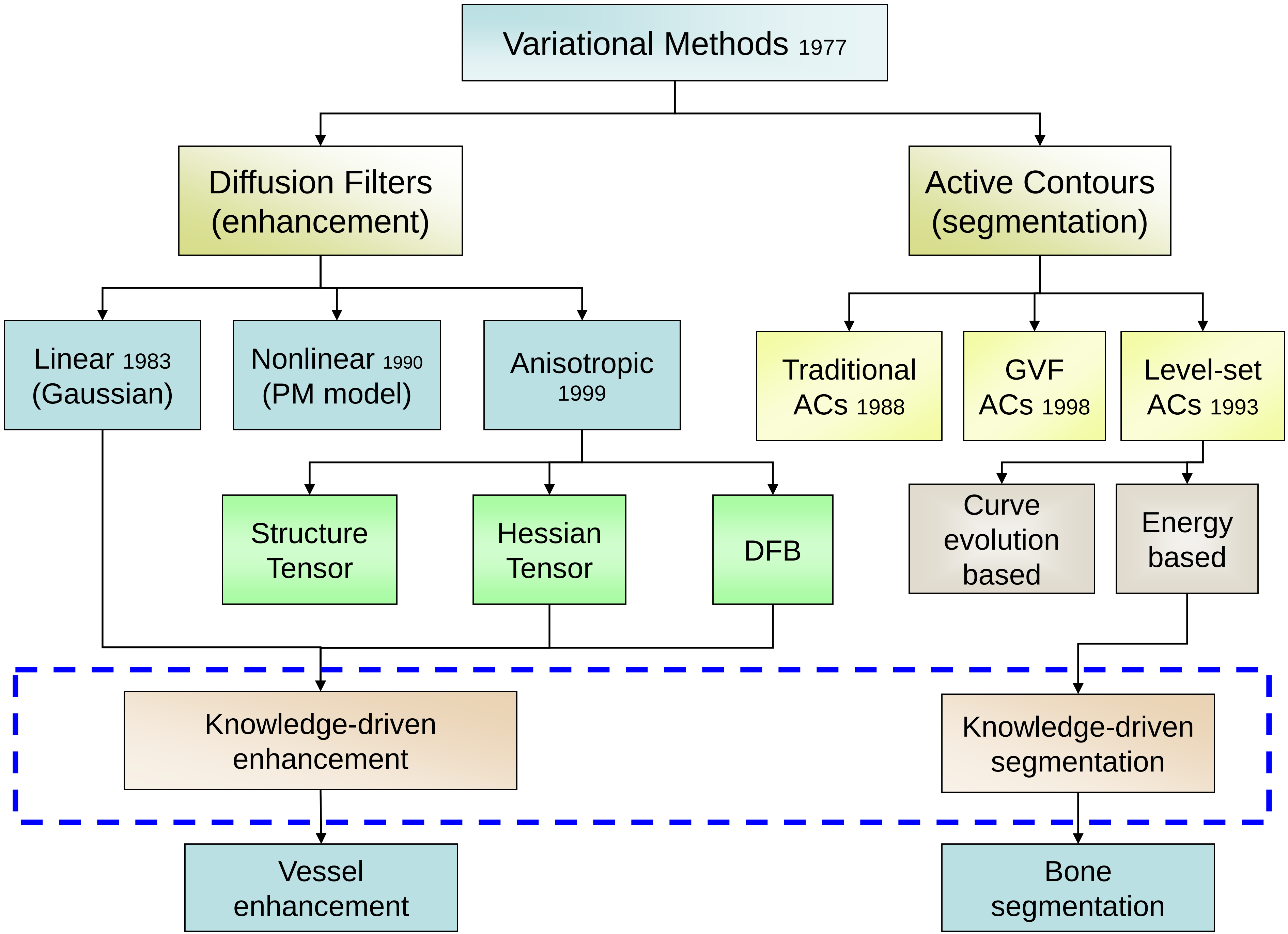
Variational Methods 1977
Diffusion Filters (enhancement)
Active Contours (segmentation)
Linear 1983 (Gaussian)
Nonlinear 1990 (PM model)
Anisotropic 1999
Traditional ACs 1988
GVF ACs 1998
Level-set ACs 1993
Structure Tensor
Hessian Tensor
DFB
Curve evolution based
Energy based
Knowledge-driven enhancement
Knowledge-driven segmentation
Vessel enhancement
Bone segmentation

Diffusion Filter

- Takes name from physical diffusion process
- To smooth an image I using heat equation (iterative process)

$$\frac{\partial I(\mathbf{x},t)}{\partial t} = \mathrm{div}\left(D \cdot \nabla I\right)$$

- $D = 1$: linear
- $D = g(\mathrm{x})$: $R^2 \rightarrow R$: nonlinear
- D = matrix: anisotropic

Linear Diffusion and Scale Space

$$\partial_t I = \mathrm{div}\left(\nabla I\right) = \Delta I$$

- Stopping the linear diffusion process after a time t = Gaussian filtering with a scale **$\sigma = (2t)^{0.5}$**.
- Let t vary from 0 to ∞, one obtains a ***scale-space*** for the image: a family of gradually smoother versions of it.
- **Scale-space analysis** is natural in vision because objects become larger when we move closer to them and vice versa.

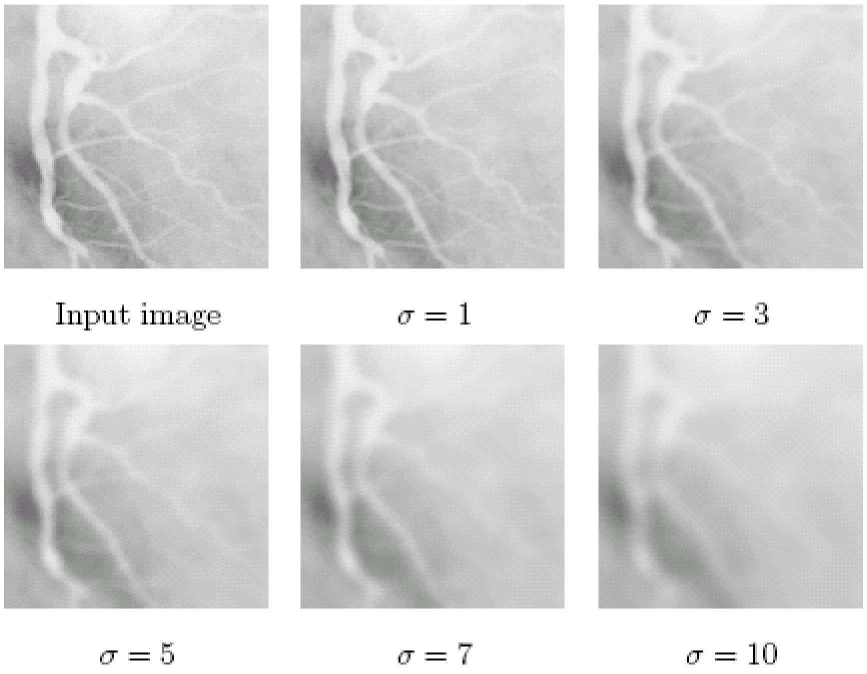

Gaussian smoothing with various scales. Note how small vessels are gradually removed

Nonlinear Diffusion

- Perona-Malik model: $D = g(|\nabla I|)$ an edge function.

$$\partial_t I = \mathrm{div}\left(g(|\nabla I|)\nabla I \right)$$

$$g(|\nabla I|) = \frac{1}{1 + |\nabla I|^2 / \lambda^2}$$

  – $g \rightarrow 0$ when $|\nabla I| \rightarrow \infty$ (at edges)
  – $g \rightarrow 1$ when $|\nabla I| \approx 0$ (homogenous structures)

- Removing noises while preserving edges.

Anisotropic Diffusion

- Nonlinear diffusion: stops smoothing at edges.
- In some applications, it is desirable to stop smoothing across edges only while maintaining the smoothing along edges → introducing a ***diffusion tensor D***:
  - its eigenvectors define directions for smoothing, estimated using ***structure tensor ST***
  - its eigenvalues define the amount of smoothing in the corresponding directions

Input image

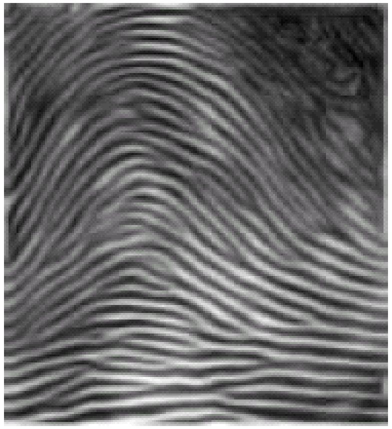

Filtered image

Noise is removed while coherence is enhanced

$$ST = \begin{bmatrix} I_x^2 & I_x I_y \\ I_x I_y & I_y^2 \end{bmatrix}$$

Hessian-based Filters

- Structure analysis using Hessian tensor.
  - A line-like structure model incorporated.

$R = |\lambda_1/\lambda_2|$ small → lines
large → others

$$\psi_\sigma(\mathbf{x}) = \mu . e^{-\frac{R^2}{2\beta^2}}$$

- Scale space analysis: to detect various line's width.
  - σ varies in a range S
  - $\max_{\sigma \in S} \{\psi_\sigma(x)\}$ is selected

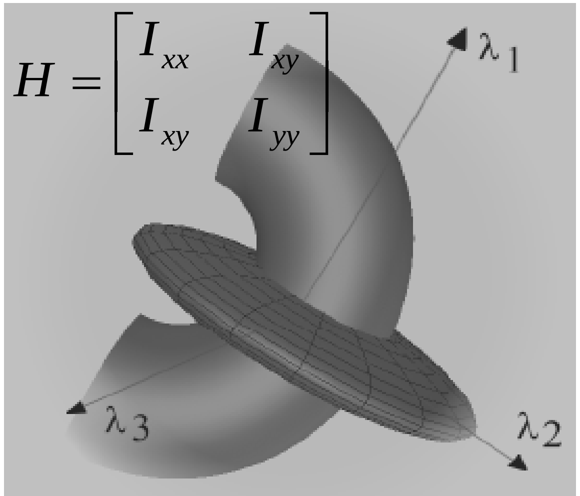

Hessian eigenvalues

Application: vessel enhancement

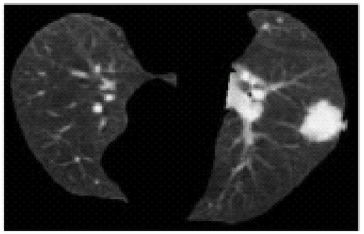
Input image

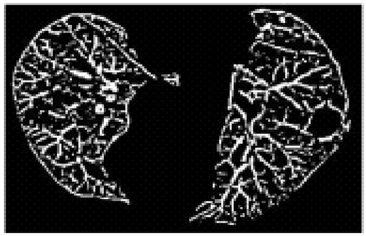
Enhanced image

Problems of Hessian-based Filters

- A line has one principal direction
  - Noises have more than one principal direction → large R → suppressed.
- Problems:
  - Junctions will be suppressed too,
  - Second derivatives are noise sensitive.

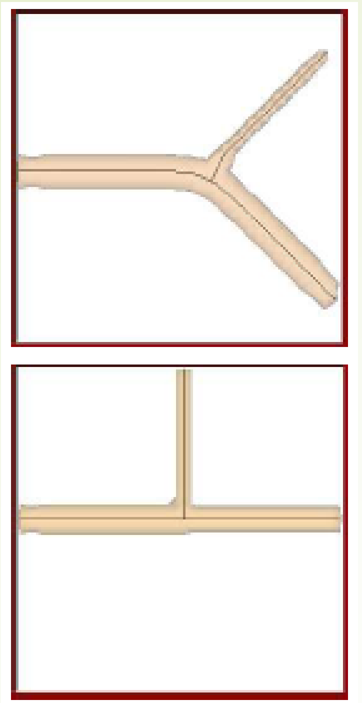

Junctions have more than one direction

Original image Frangi filter Shikata filter

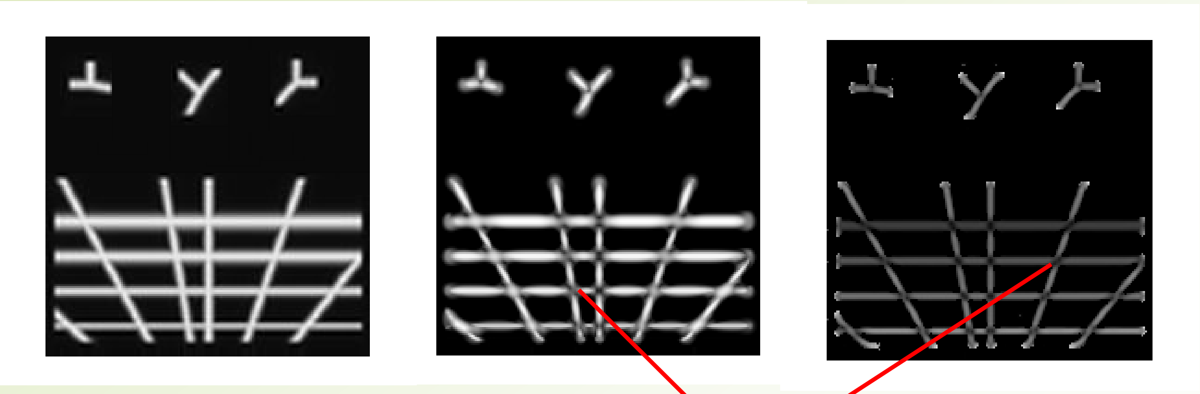

Junctions suppressed

DFB-based Filter

I propose to replace the direction estimation (through the Hessian analysis) by a directional decomposition of the input image.

- Information about direction of a vessel is available in directional images.
- Noises in directional images is reduced due to its omni-directional nature.

The advantage of the proposed approach is that it distinguishes all vessels at bifurcations and crossings and is less sensitve to noise.

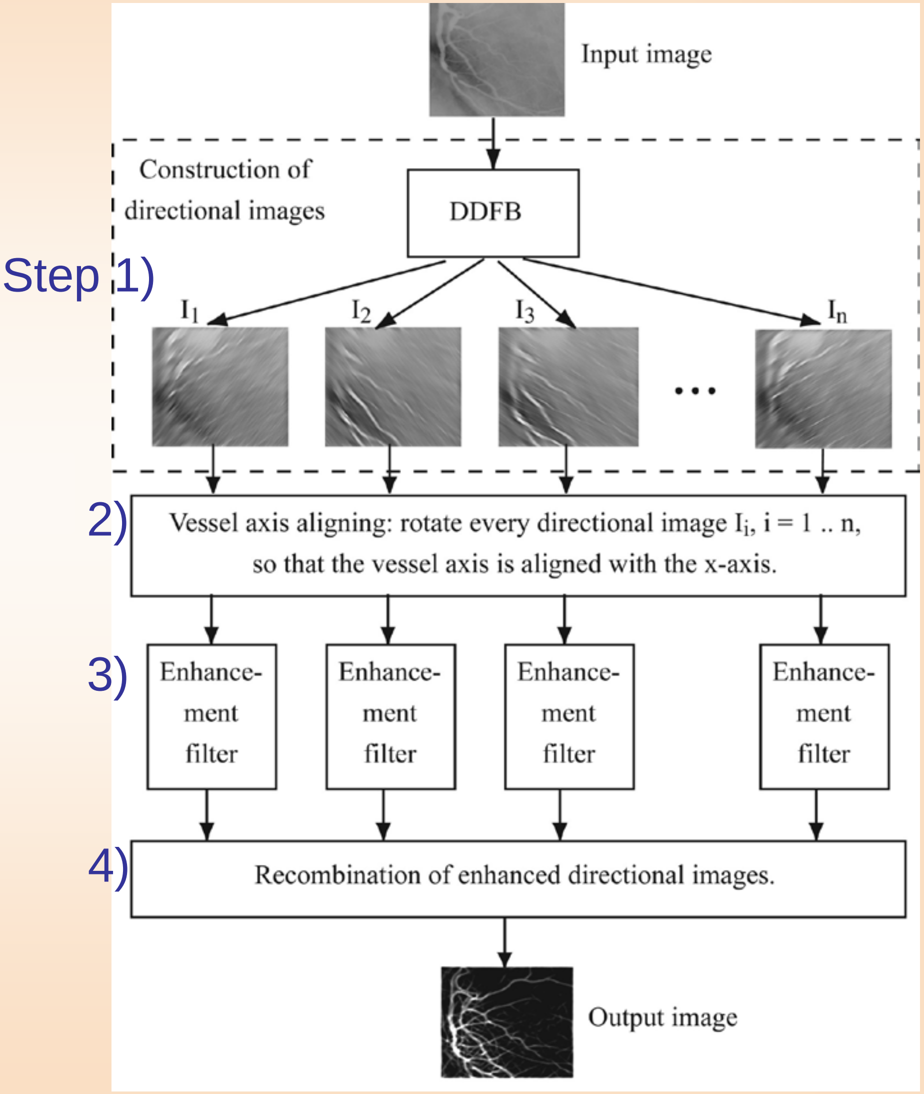

Diagram of the proposed filter

Evaluation

➢ Testing Data

- One phantom image with different kinds of junctions.
- Two real cardiac angiography images without known ground truths (qualitative only).
- 40 retinal images with GTs known (Utrecht database).
- A set of 615 noisy images (1 phantom + 40 Utrecht images x 15 noise levels each).

➢ Evaluation Method

- ROC (receiver operating curve).
- The closer the curve approaches the top left corner, the better the classification → reflected by the area under the curve (AUC)

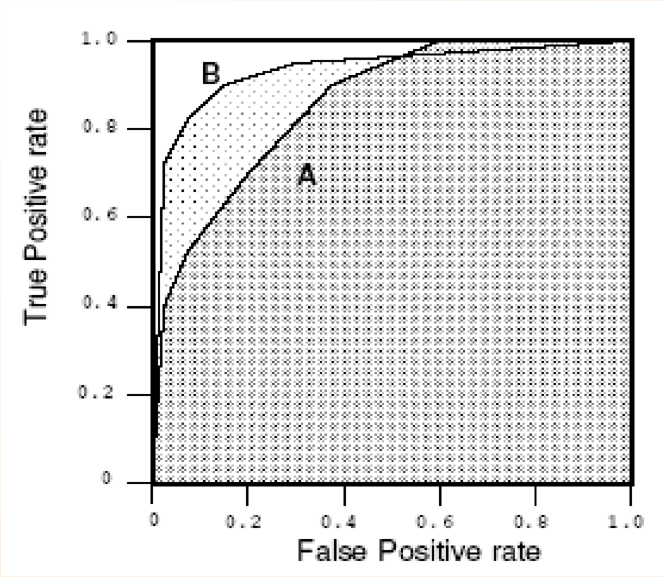

Two ROC curves. B is better than A

Experimental Results

- Junction suppression:
  - Synthetic image with various types of junctions

Original images | Frangi results | Shikata results | Our results

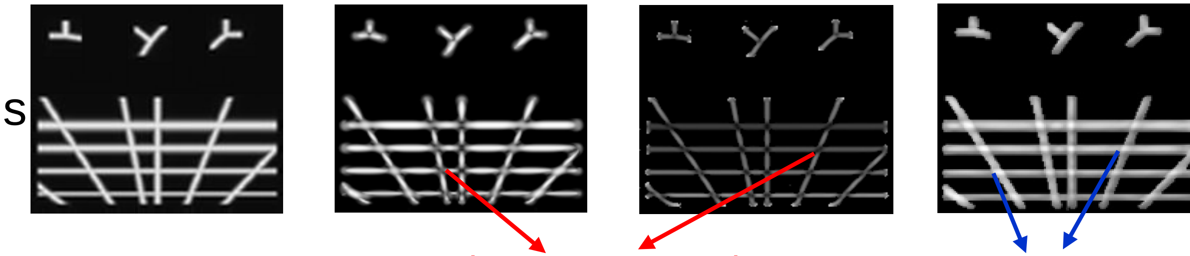

Junctions suppressed

Junctions preserved

- Noise sensitivity:
  - 40 images x 15 noise levels each

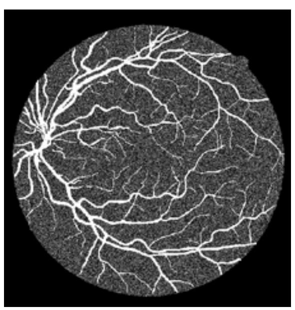

Noise std 5%

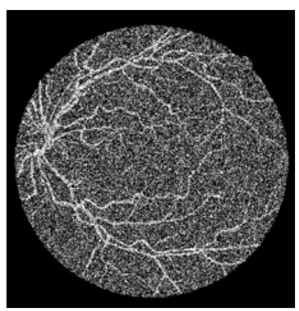

80%

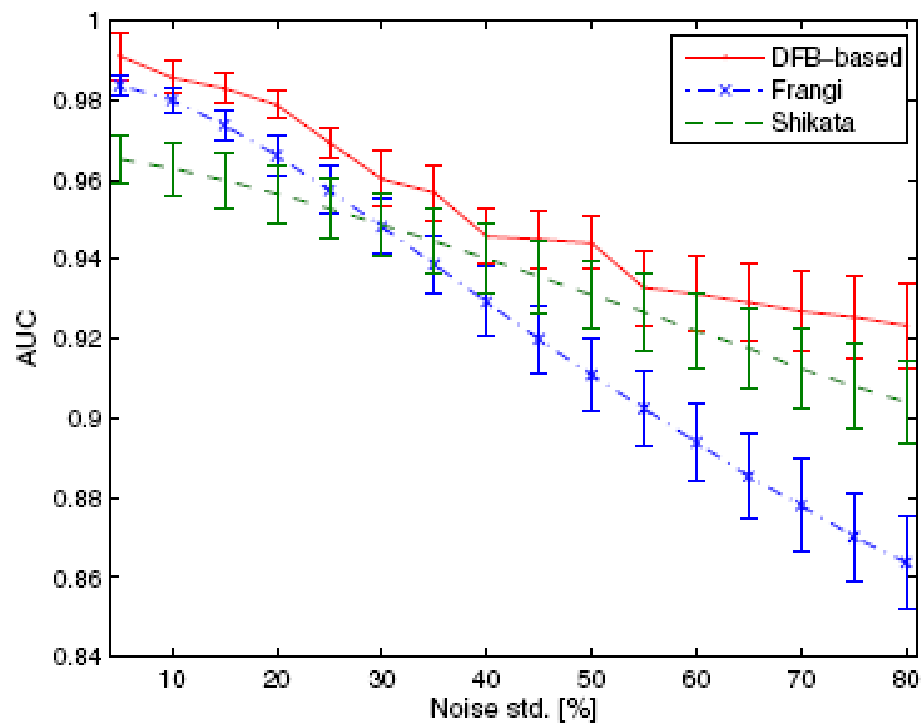

Performance comparison of the three approaches. Our DFB-based filter outperforms the others.

Experimental Results (cont')

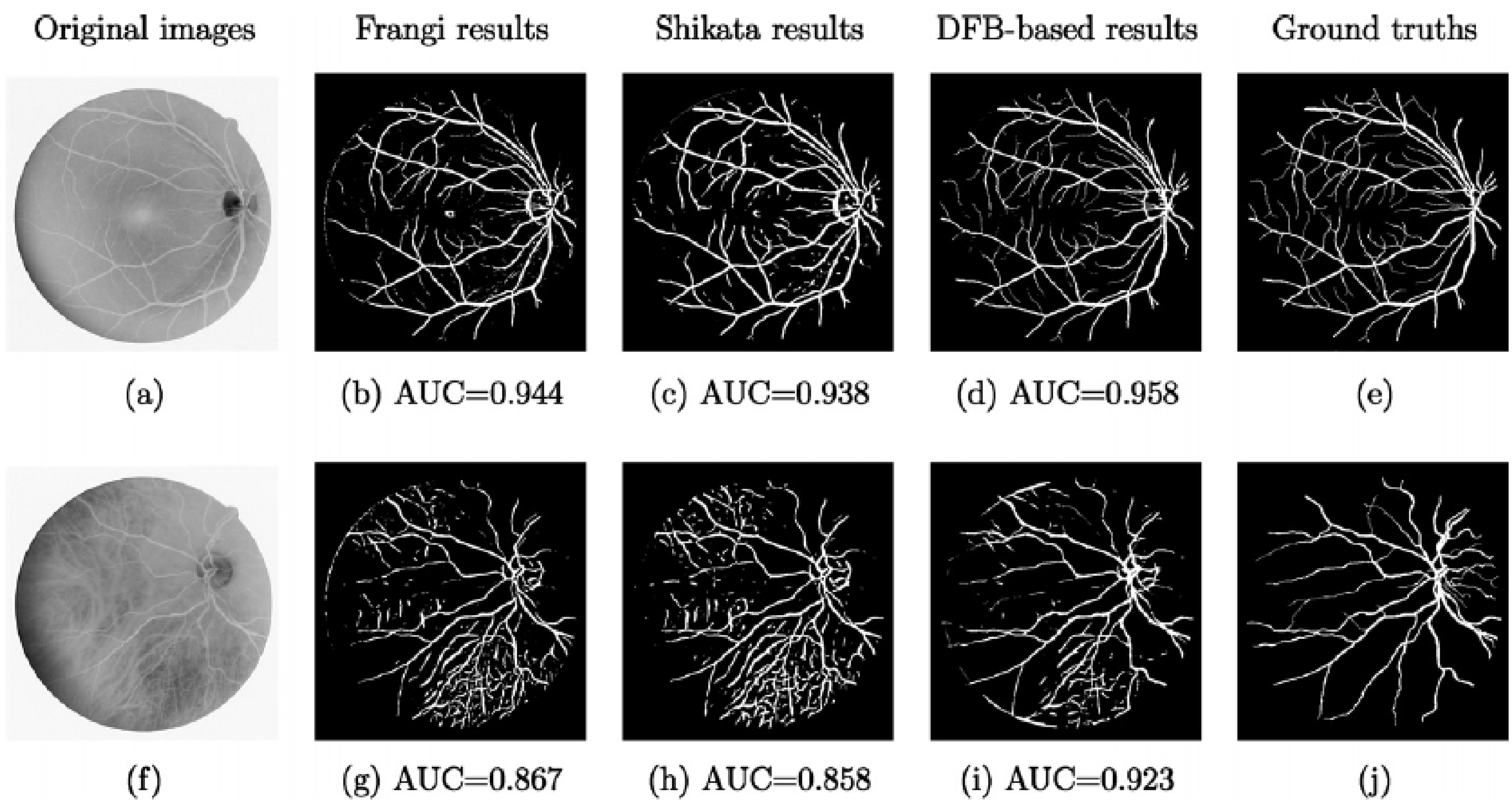

Fig. 14. Best and worst results for the Utrecht database in terms of AUC measures. For each image, the Frangi method cpu = 87.02 s, Shikata 85.55 s, and DFB-based 93.46 s.

Mean and SD of the AUC of the three methods performed on the Utrecht database

	Frangi	Shikata	DFB-based
Mean	0.8994	0.8970	0.9519
SD	0.0162	0.0152	0.0060

Discussions

- Estimation of the vessel directions without the Hessian eigen-analysis.
- Overcoming the junction suppression, which can cause serious problem from a clinical perspective (discontinued vessel tree) despite small errors from a computing perspective.
- Better non-uniform illumination removal using homomorphic filters on directional images.
- The larger the number of directional images, the more accurate the eigenvalue estimation is, at the cost of the computation time.
- Can be extended to deal with 3D images by extending DDFB to 3D, which is our future work.

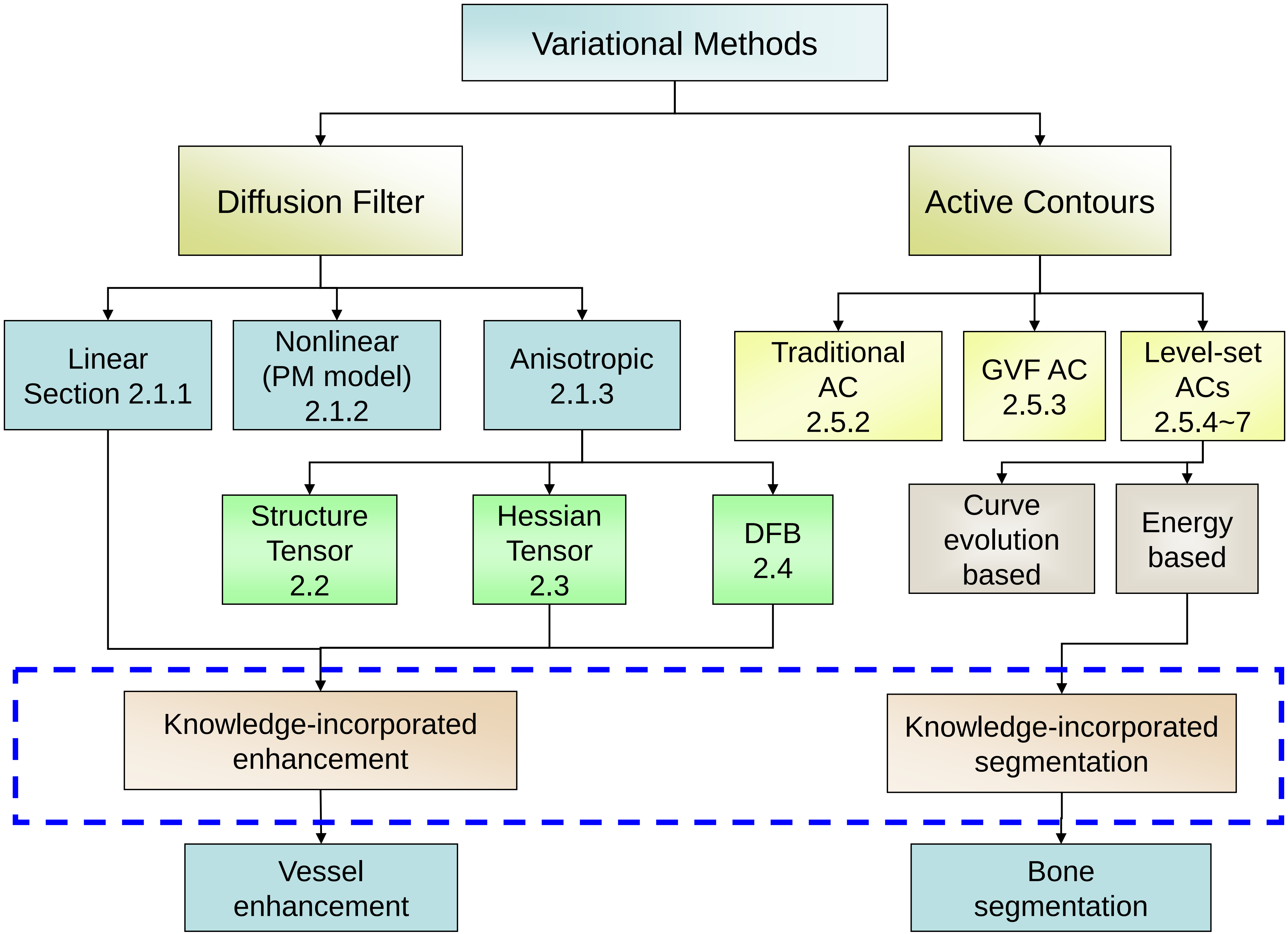
Variational Methods
Diffusion Filter
Active Contours
Linear
Section 2.1.1
Nonlinear
(PM model)
2.1.2
Anisotropic
2.1.3
Traditional
AC
2.5.2
GVF AC
2.5.3
Level-set
ACs
2.5.4~7
Structure
Tensor
2.2
Hessian
Tensor
2.3
DFB
2.4
Curve
evolution
based
Energy
based
Knowledge-incorporated
enhancement
Knowledge-incorporated
segmentation
Vessel
enhancement
Bone
segmentation

Active Contours

- A less local method to handle edges.
- Sometimes called **snakes** or **deformable models**.
- Description of contours which evolve under appropriate forces to move towards edges.
- Issues:
  - initialization,
  - false edges,
  - topology changes.

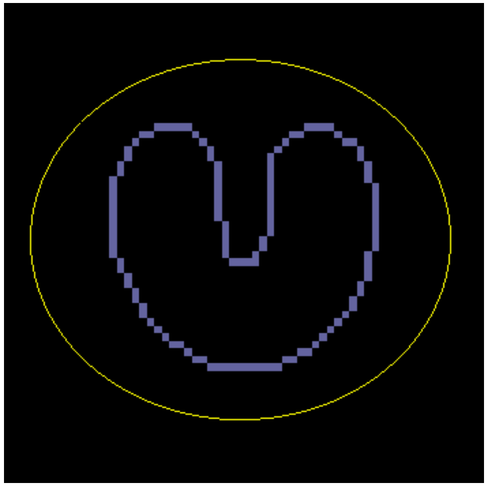

Snake evolution

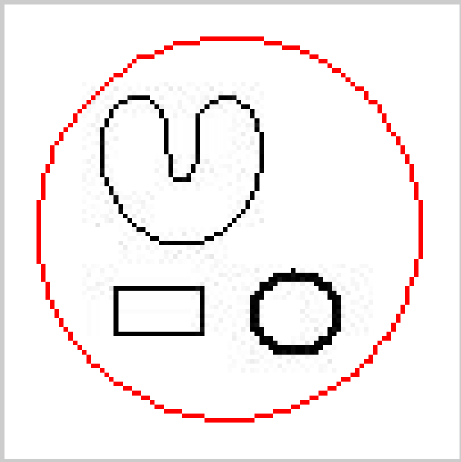

Topo-unadaptability video

Level-set Methods

- Curve is embedded as the zero level set.
- $C = \{(x,y) \mid \phi(x,y) = 0\}$

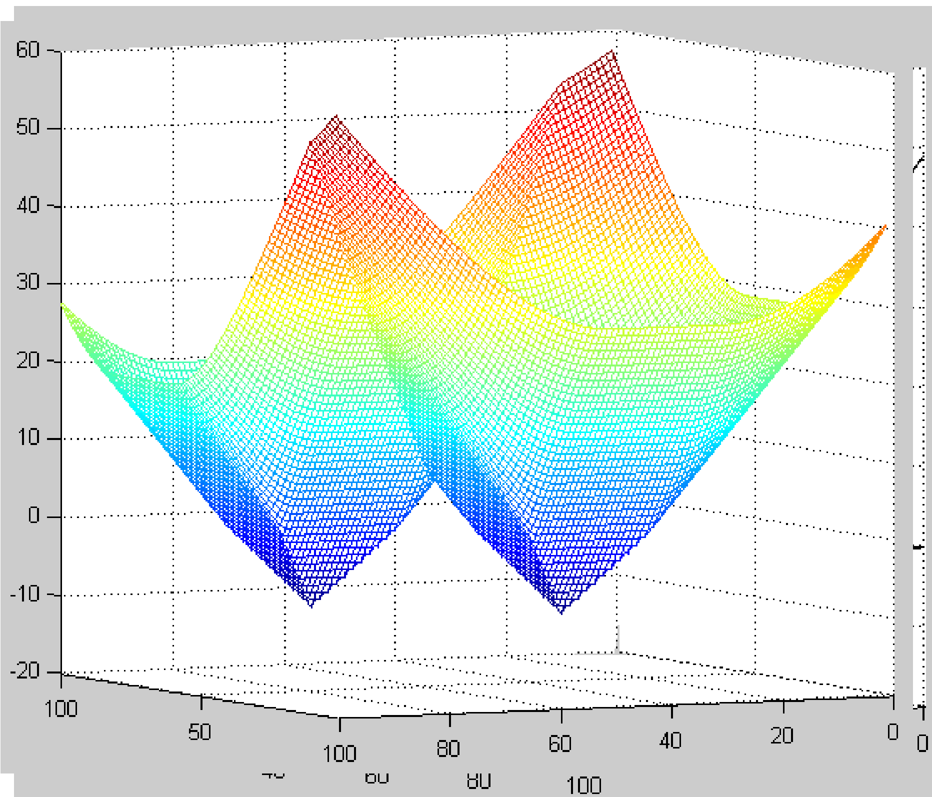

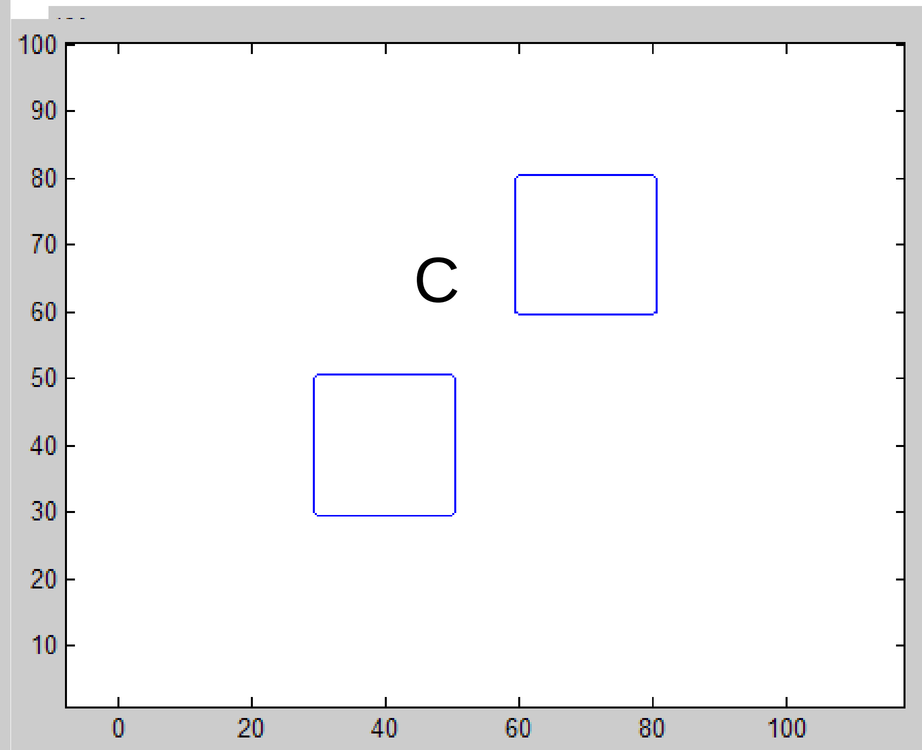

Evolution Forces

- Types of forces
  - A force in the normal direction to the curve
  - An external vector field
  - A force based on the curvature of the curve.

- Partial Differential Equation:

$$\frac{\partial \phi}{\partial t} + \underbrace{\vec{S} \cdot \nabla \phi}_{\text{Vector Field Based}} + \underbrace{V_N \left| \nabla \phi \right|}_{\text{In Normal Direction}} = \underbrace{b\kappa \left| \nabla \phi \right|}_{\text{Curvature Based}}$$

$$\boxed{\text{parameters: } \left(b, V_N, \vec{S} \right)}$$

Force in Normal Direction

- All level sets of $\phi(x,y)$ are evolving.
- We only track zero level set.

$$\frac{\partial \phi}{\partial t} + V_N \left| \nabla \phi \right| = 0 \qquad V_N = 1$$

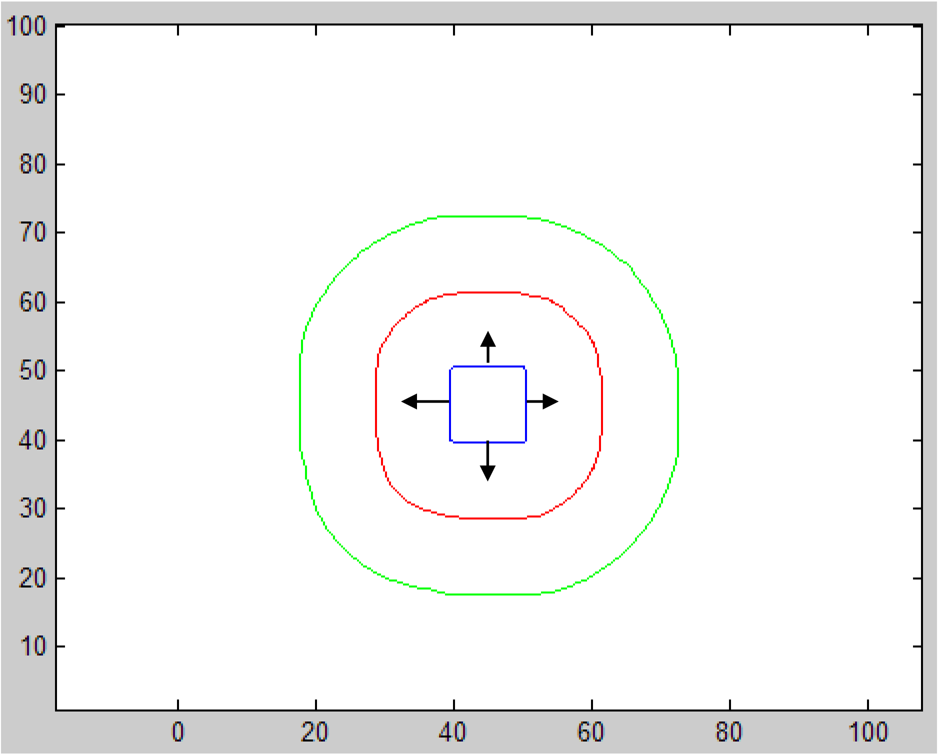

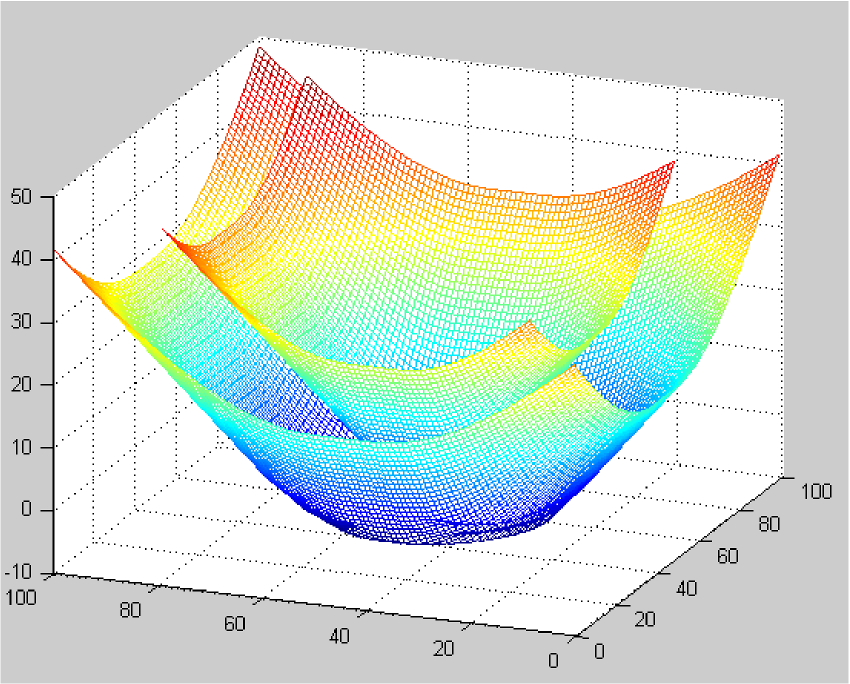

External Vector Field

$$\frac{\partial \phi}{\partial t} + \vec{S} \cdot \nabla \phi = 0$$

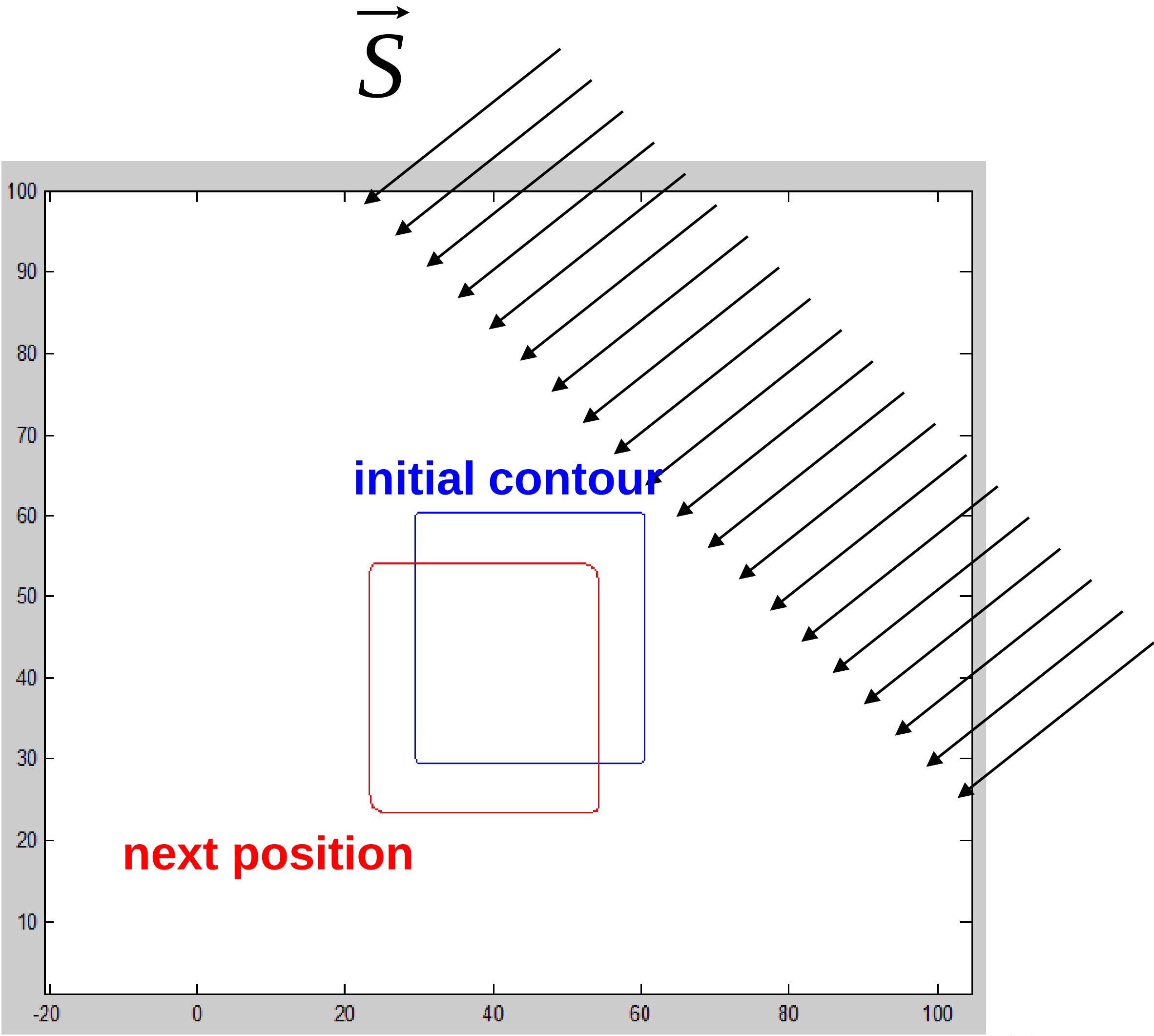

Simultaneous Translation and Expansion

$$\frac{\partial \phi}{\partial t} + \vec{S} \cdot \nabla \phi + V_N \left| \nabla \phi \right| = 0$$

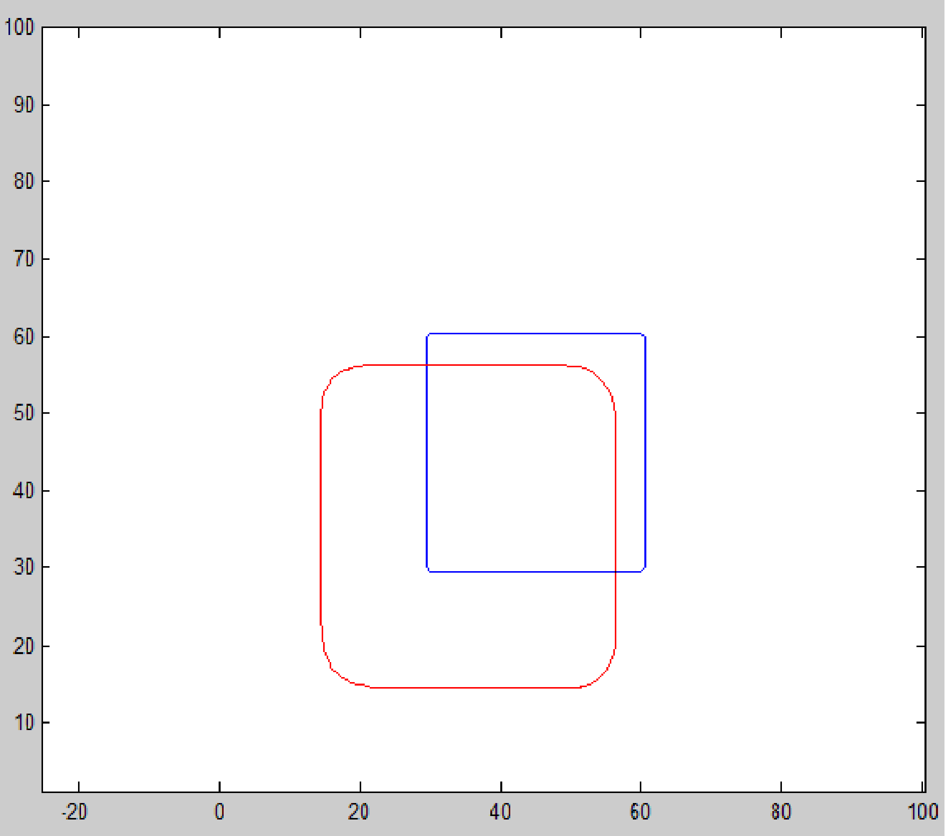

Curvature-based Force

- Smoothing the contour.

$$\frac{\partial \phi}{\partial t} = b\kappa \left| \nabla \phi \right|$$

$$\text{where } \kappa = \text{div}\left(\frac{\nabla \phi}{\left| \nabla \phi \right|} \right)$$

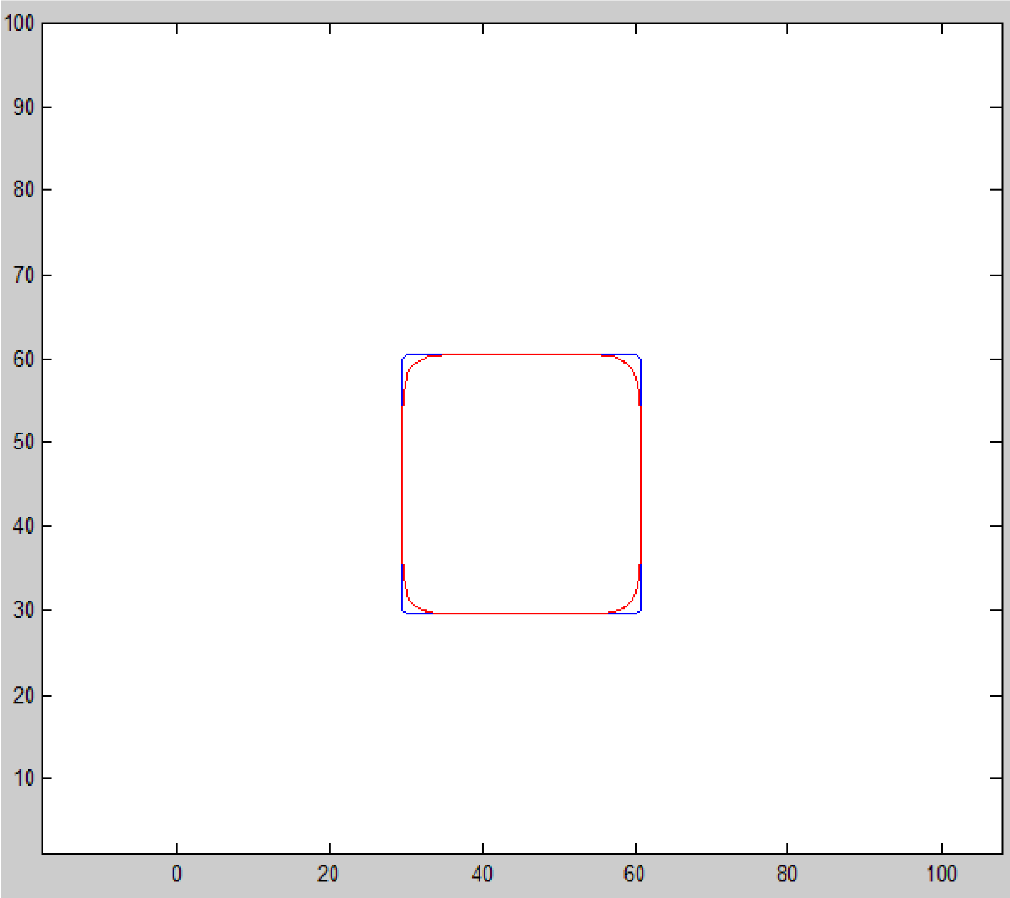

Curvature-based Force

$b = 1$

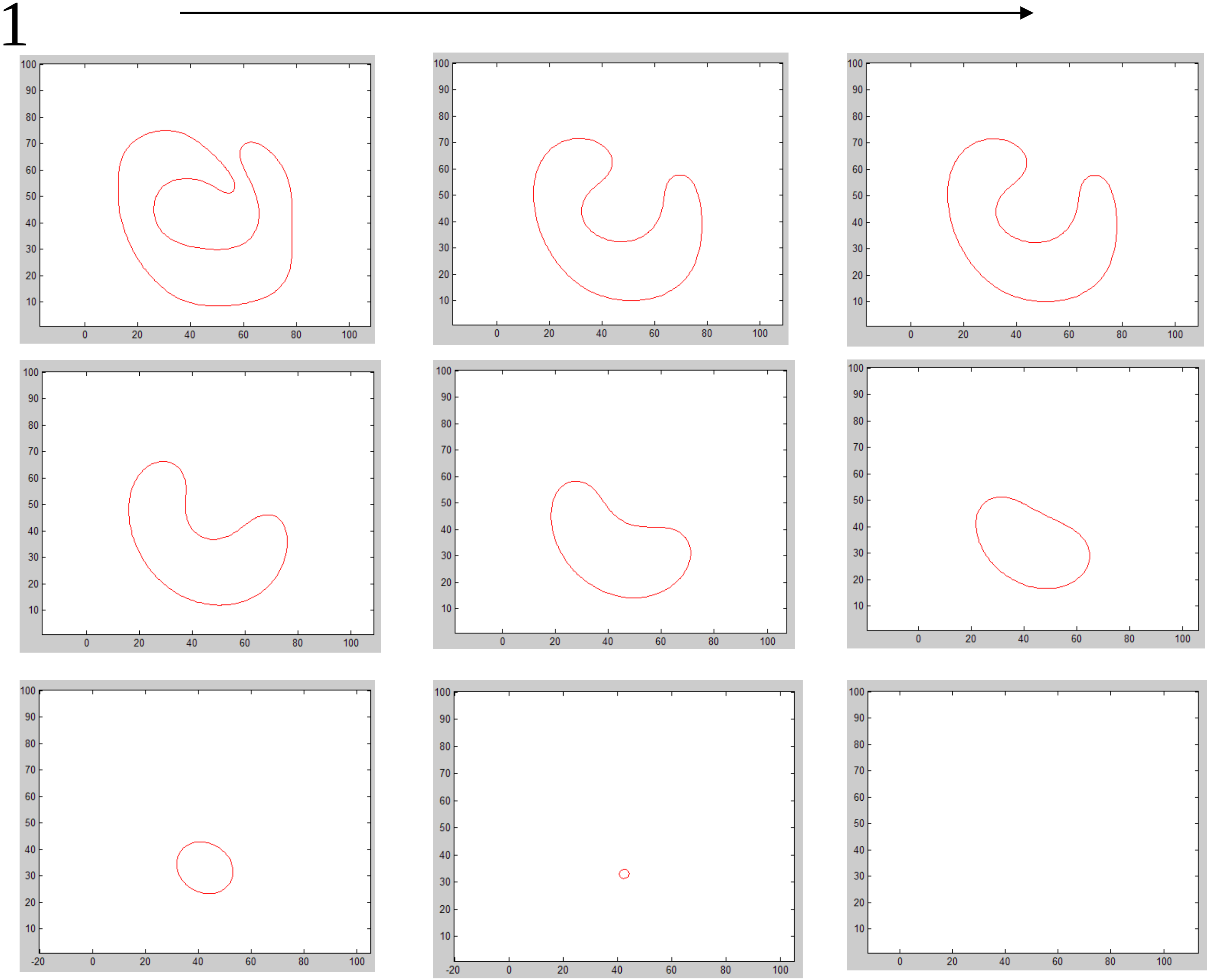

Topological Changes

- Topological changes such as merging and splitting are handled naturally by Level-set Methods

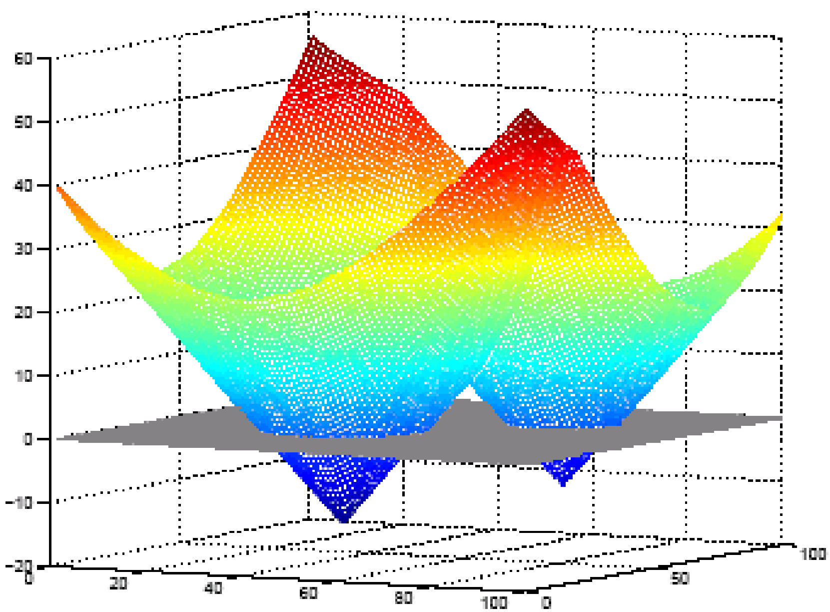

Level-set function ϕ

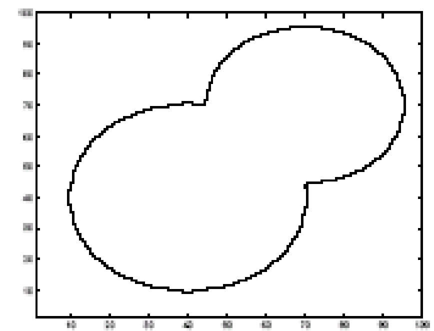

Initial zero level set

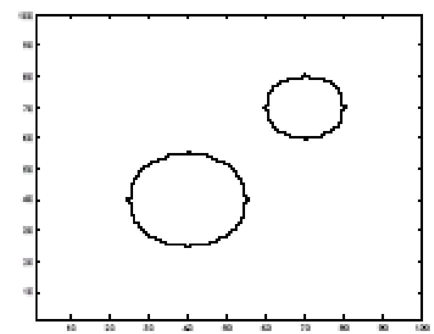

Zero level set after evolution

Geometric AC

$$\partial_t \phi = g.\left(\kappa + V_0\right).|\nabla \phi|$$

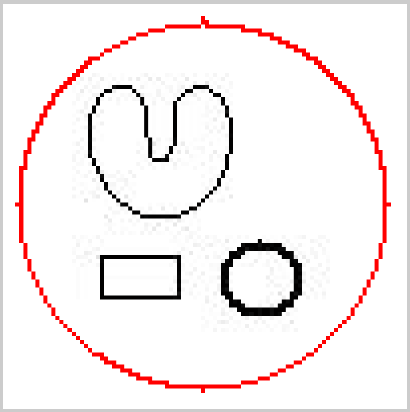

Topo-adaptability video

- That is,

$$b = g(x)$$
$$V_N = V_0 g(x)$$
$$\vec{S} = 0$$

- $g = g(\mathrm{x}) = g(|\nabla I|)$: edge function (small at edges and large otherwise)
  - similar to that in nonlinear diffusion, e.g.,

$$g(|\nabla I|) = \frac{1}{1 + |\nabla I|^2 / \lambda^2}$$

Geodesic AC

- In order to detect an object, one can search for the path of minimal edge-weighted length

$$L_R = \int_C g\left(|\nabla I(C(s))|\right) ds$$

- Leading to $\partial_t \phi = g.(\kappa + V_0).|\nabla \phi| + \nabla g \cdot \nabla \phi$
- That is, $b = g(x)$

$$V_N = V_0 g(x)$$

$$\vec{S} = \nabla g$$

- The last term is used to increase the curve attraction towards weak edges (or gaps).

GVF-Geometric AC

Gradient

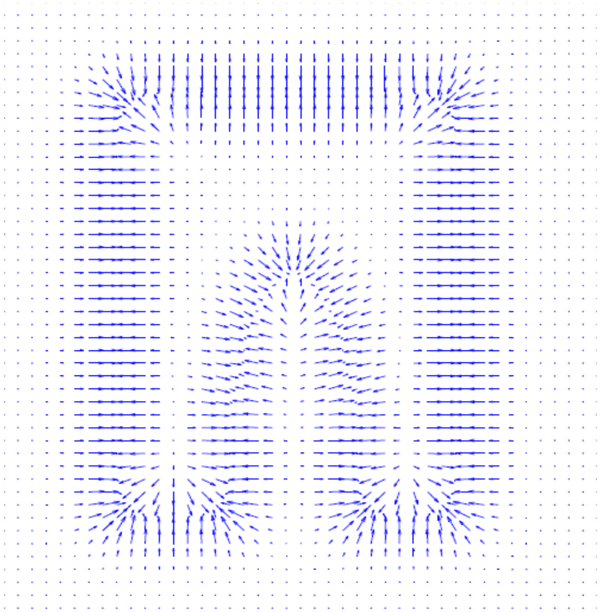

∇g

Gradient vector flow (GVF) by Xu and Prince

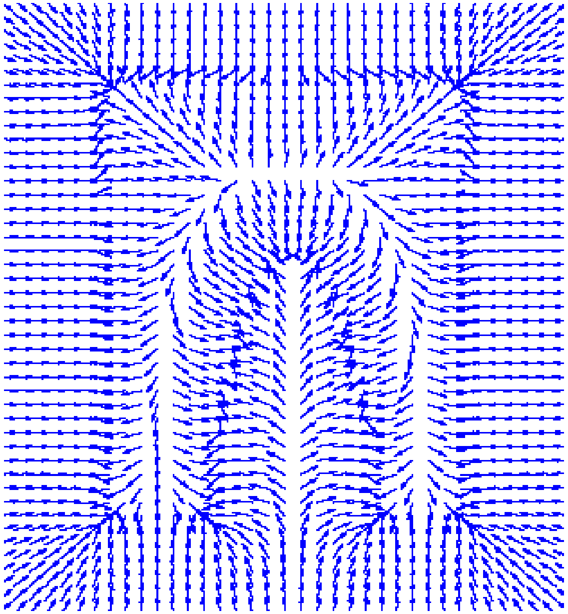

$[\hat{u}, \hat{v}]$

Replacing ∇g by $[\hat{u}, \hat{v}]$

$$\partial_t \phi = g\left\{(\kappa + V_0)\,|\nabla \phi| - [\hat{u}, \hat{v}] \cdot \nabla \phi\right\}$$

That is,

$$b = g(x)$$

$$V_N = V_0 g(x)$$

$$\vec{S} = [\hat{u}, \hat{v}]\, g(x)$$

Chan-Vese AC

- Chan-Vese (CV) energy functional

$$F(C) = \int_{\text{inside}(C)} \left| I(x) - c_{in} \right|^2 dx + \int_{\text{outside}(C)} \left| I(x) - c_{out} \right|^2 dx$$

c_{in} and c_{out} are mean values inside and outside the curve C.

- Leading to

$$\partial_t \phi = |\nabla \phi| \left[\nu\kappa + V_0 + (I - c_{in})^2 - (I - c_{out})^2 \right]$$

- That is,

$$b = \nu = const$$

$$V_N = V_0 + \left[\left(I - c_{in}\right)^2 - \left(I - c_{out}\right)^2 \right]$$

$$\vec{S} = 0$$

- Does not depend on edge function *g*.

Connection: Diffusion Filters and ACs

- Geodesic AC flow

$$\partial_t \phi = |\nabla \phi| \operatorname{div}\left(g(I) \frac{\nabla \phi}{} \right)$$

depends on two functions: ϕ and I

- Consider the case $\phi = I$, lea

ik dif

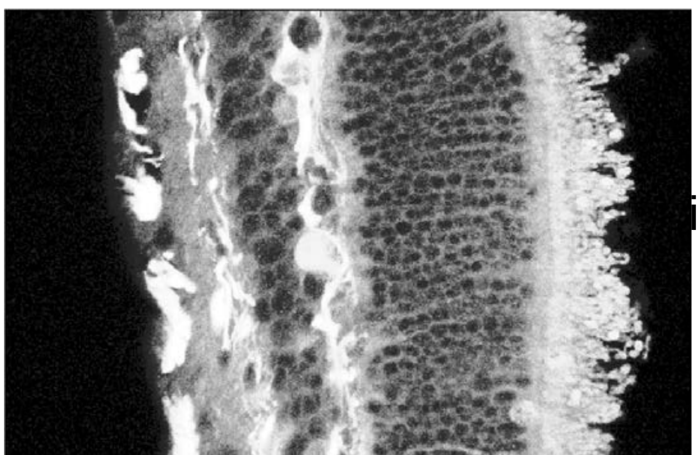

I

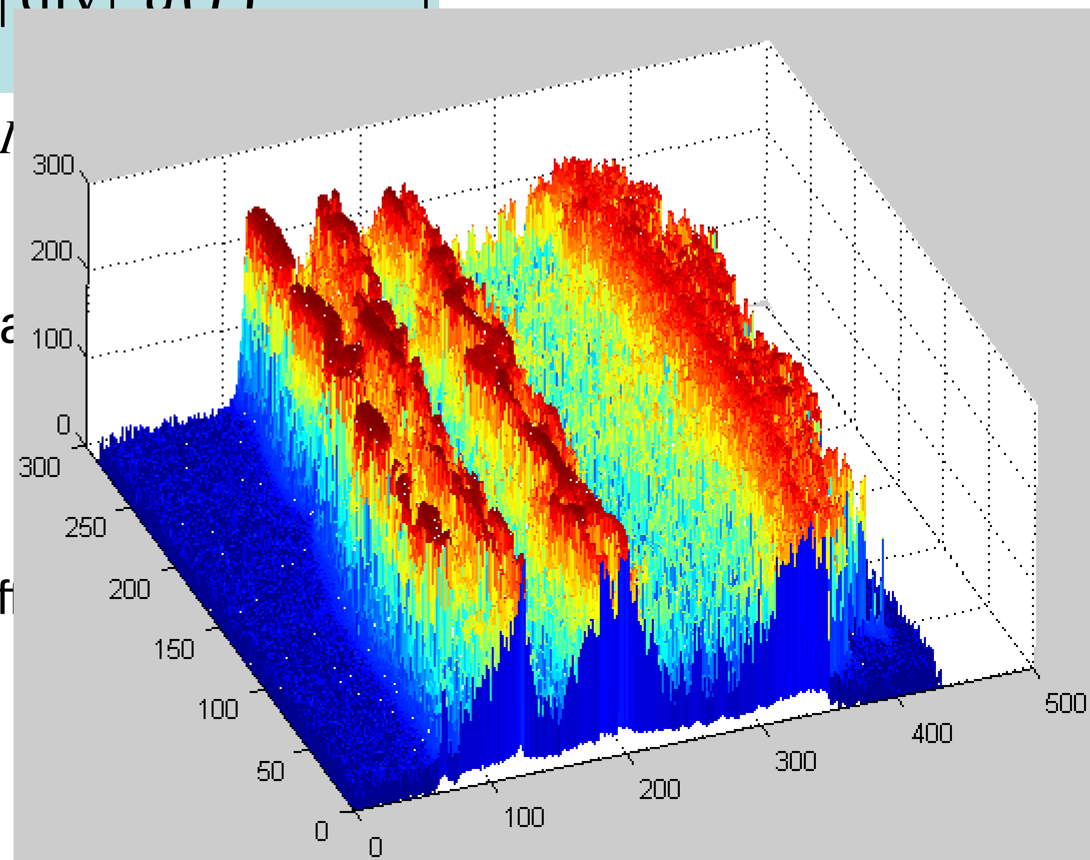

$\phi = I$

Self-snake

Original image

After 10 iterations

After 30 iterations

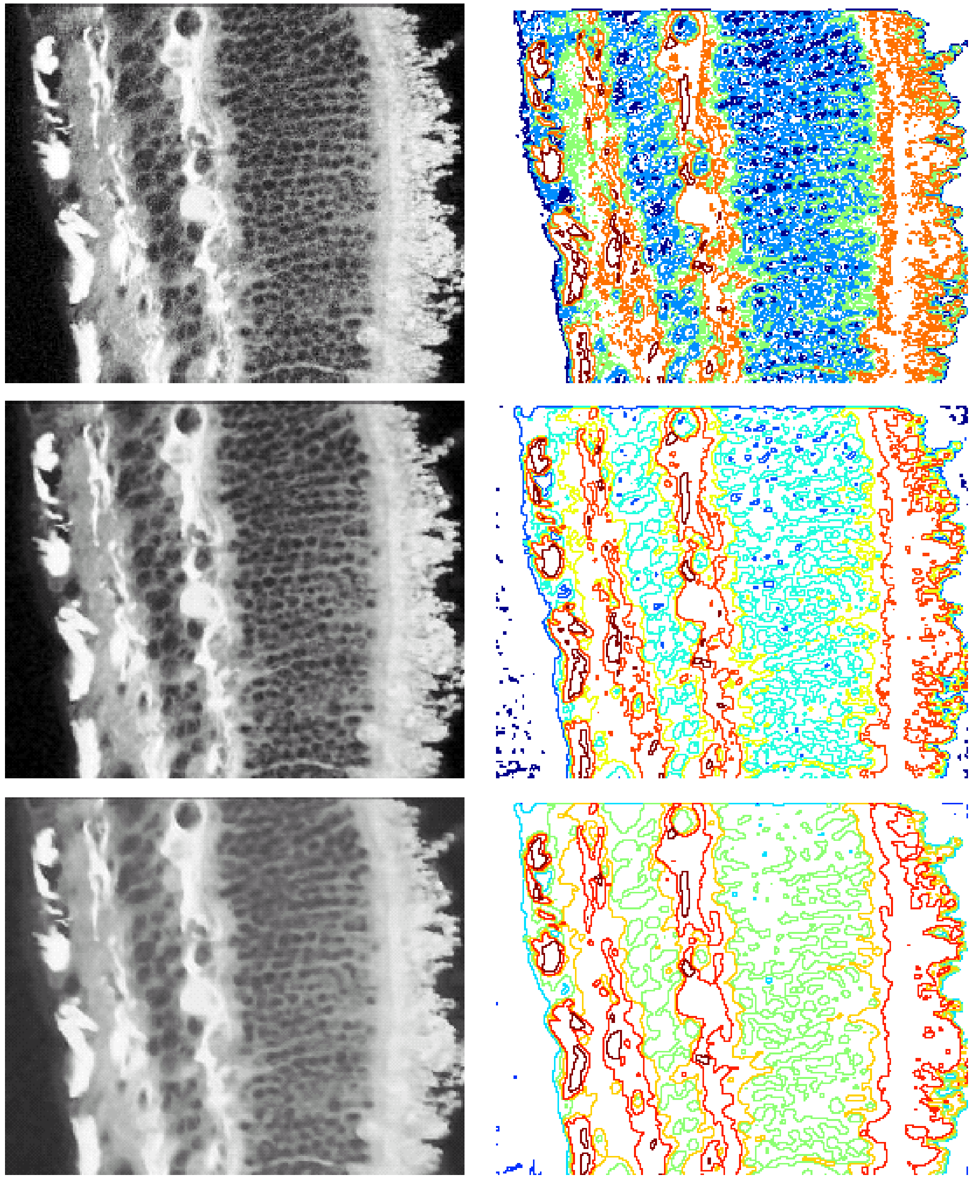

Images Corresponding level sets

Denoising using self-snake model

Bone Segmentation

Bone segmentation from CT images

- **critical component** in computer-assisted orthopedic surgery
- **challenging task** due to inhomogeneous bone structures, low contrast edges, and overlapping intensity values of bones.

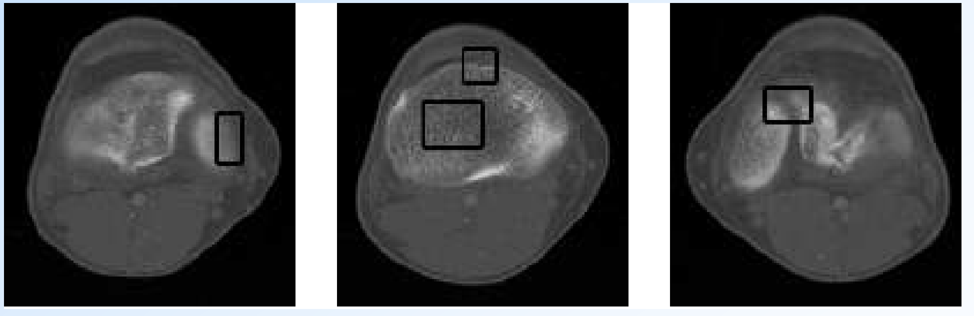

Typical CT bone images with challenging obstacles for accurate segmentation

ACs in Bone Segmentation

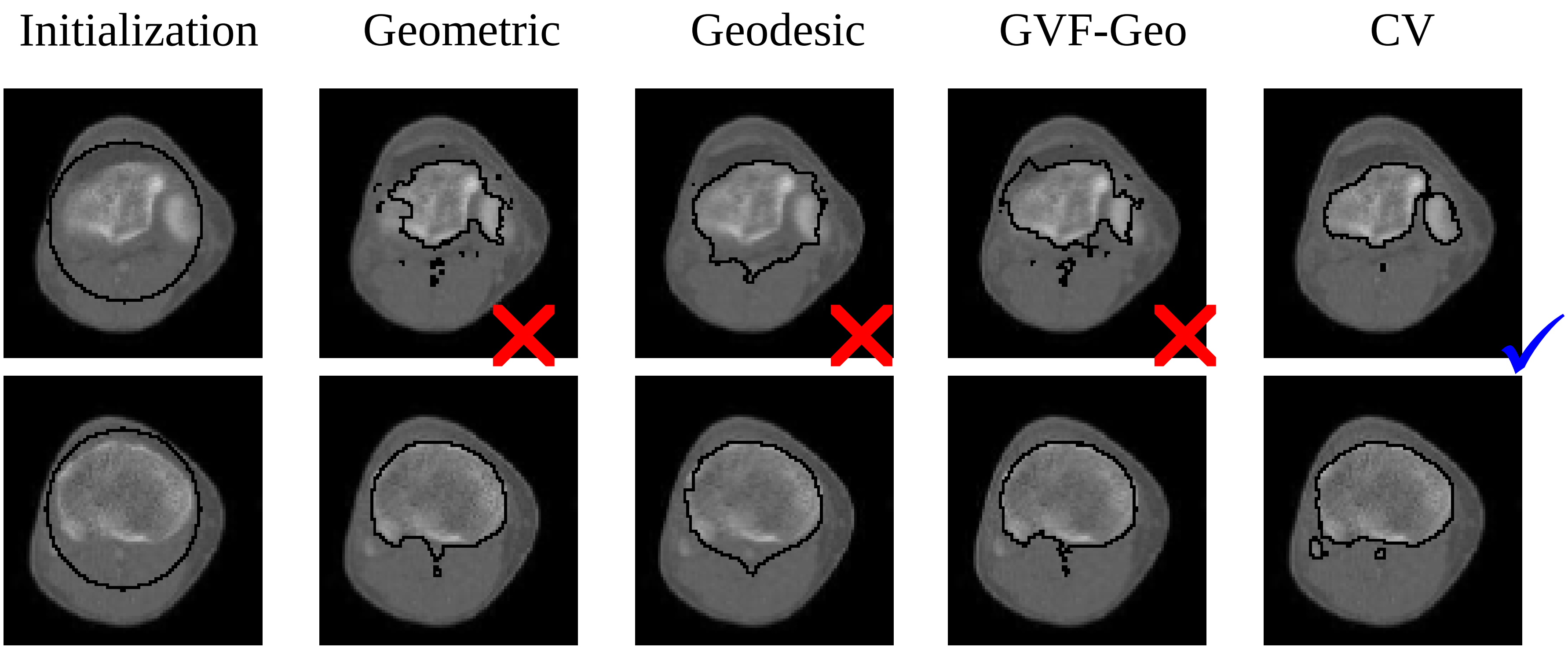

- The first three ACs: edge-based → sensitive to noise.
- CV AC: without edges → more robust to noise.

Problem of CV AC

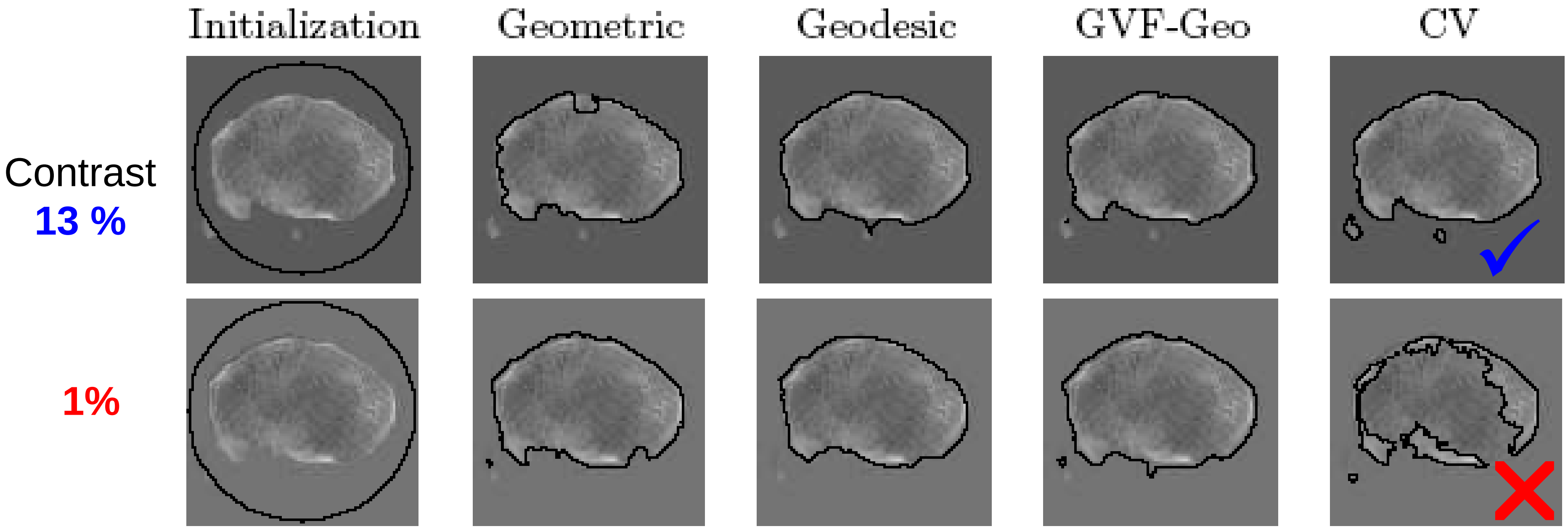

- CV AC is sensitive to contrast level.

Why CV AC Fails

- ➢ In CV energy, an object is represented by its mean value only.

$$F(C) = \int_{\text{inside}(C)} |I(x) - c_{in}|^2 \, dx + \int_{\text{outside}(C)} |I(x) - c_{out}|^2 \, dx$$

➢The global minima of the CV energy F(C) do not guarantee the “desirable” segmentation result.

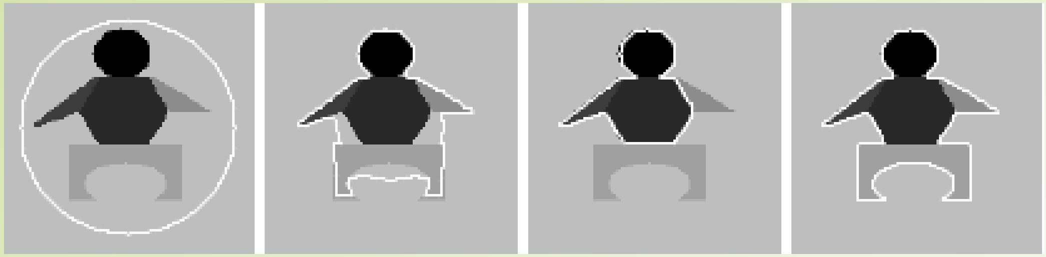

Initial, $F(C) = 645$	Intermediate, 312	Final curve, 34	Desired, 197

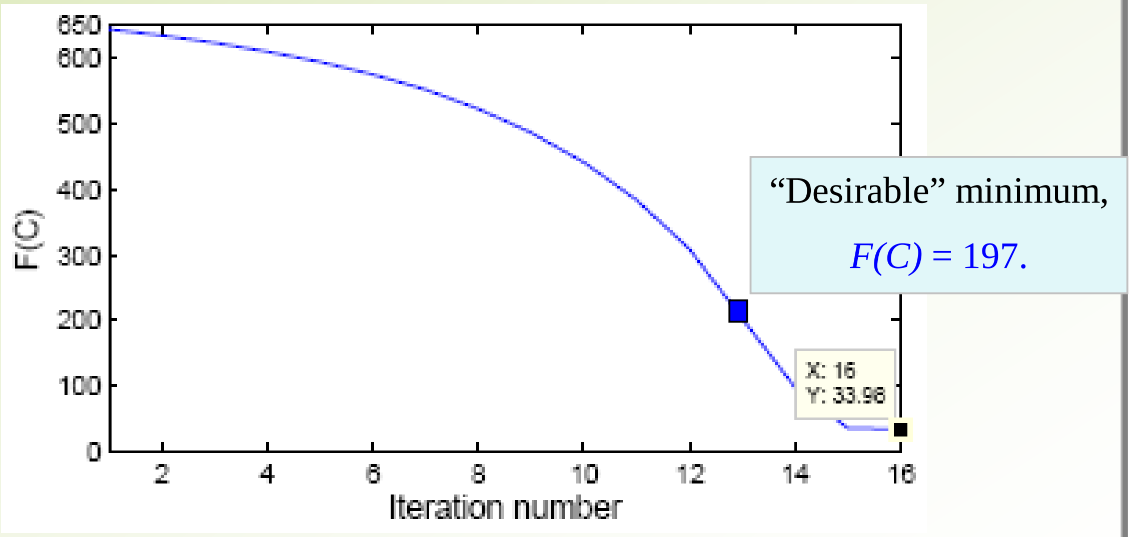

Plot of *F(C)* vs. iteration number.
The obtain minimum (34) is NOT the “desirable” one (197).

Augmented CV AC

- CV AC tries to minimize the dissimilarity within each segment.

- I proposed to incorporate a Bhattacharyya distance-based term, ***B(C),*** leading to a new evolution flow that ***both minimizes the differences within each segment and maximizes the distance between distinct segments***.

$$E(C) = \beta F(C) + (1-\beta)B(C) + \gamma \mathrm{Length}(C) + V_0 \mathrm{Area}(\mathrm{inside}(C))$$

where $B \equiv B(C) = \int_Z \sqrt{p_{in}(z)\, p_{out}(z)}\,dz$ is the Bhattacharyya coefficient, p_{in}(z) and p_{out}(z) the density functions inside and outside C, $\beta \in [0,1]$ a weighting parameter, and γ and η adjusting constants.

- The derived evolution flow:

$$\frac{\partial \phi}{\partial t} \approx |\nabla \phi| \left\{ \begin{aligned} &\gamma\kappa + V_0 + \beta\left[(I - c_{in})^2 - (I - c_{out})^2 \right] \\ &-(1-\beta)\left[\frac{B}{2}\left(\frac{1}{A_{in}} - \frac{1}{A_{out}} \right) + \frac{1}{2}\int_Z \delta(z - I)\left(\frac{1}{A_{out}}\sqrt{\frac{p_{in}}{p_{out}}} - \frac{1}{A_{in}}\sqrt{\frac{p_{out}}{p_{in}}} \right) dz \right] \end{aligned} \right\}$$

where ϕ is a level set function, $\delta(\cdot)$ the Dirac function, A_{in} and A_{out} the areas inside and outside C.

Testing Data

- A set of 16 CT images covering knee region of a patient.
  - ✓ "ground truths" drawn by a medical expert.

A real CT image with drawn GT

- Adding Gaussian noise to the GTs to have 16x5 = 80 noisy images of SNR = 10, 20, …, 50 dB.

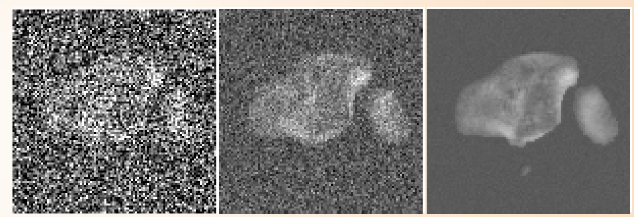

SNR 10dB 20dB 40dB

- Changing background intensity of the GTs to form 16x10 = 160 images of contrast levels varying from 1% to 20%.

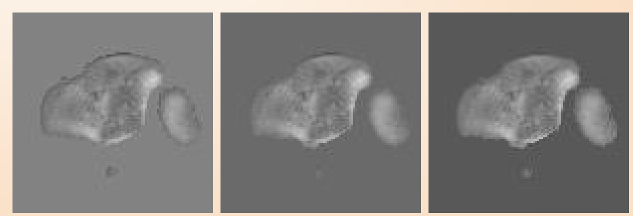

contrast 1% 11% 20%

Evaluation Method

- Two error measures:

$$\epsilon_1 = 1 - \frac{\#(Extracted\ regions \cap True\ regions)}{\#(Extracted\ regions \cup True\ regions)}$$

the relative overlap → global goodness

$$\epsilon_2 = \mathrm{Hd}(Extracted\ boundaries, True\ boundaries)$$

the difference between two contour → details of the object shape

The closer these errors to zero, the better the segmentation result.

Experimental Results

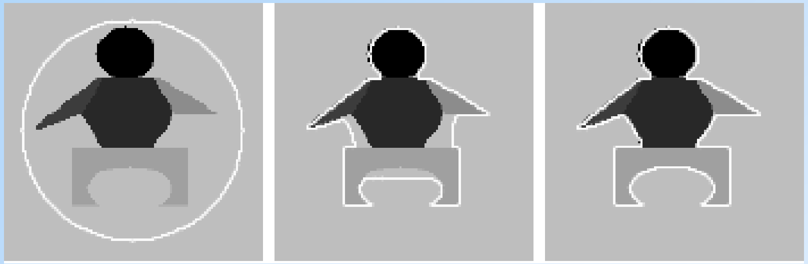

Initial, $F(C) = 645$ | Intermediate, 387 | Final curve, 196

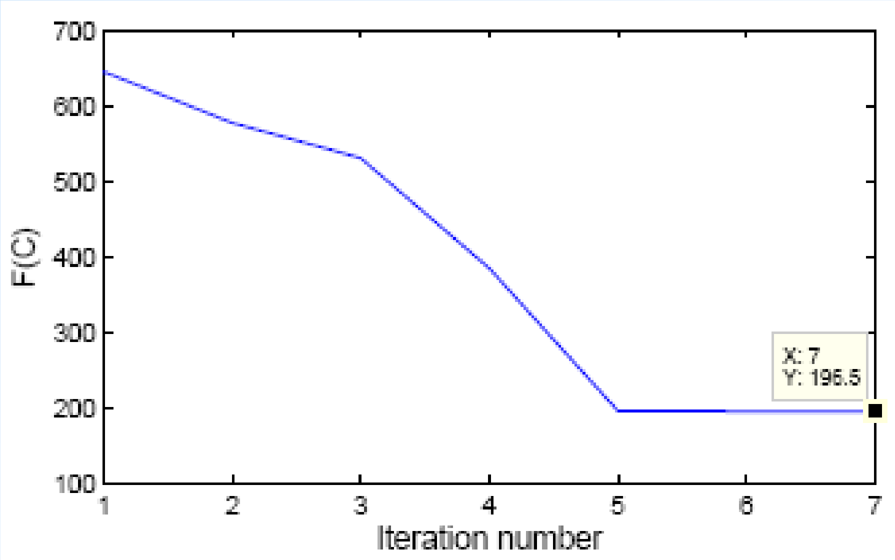

The "desirable" minimum was found.

Noise sensitivity

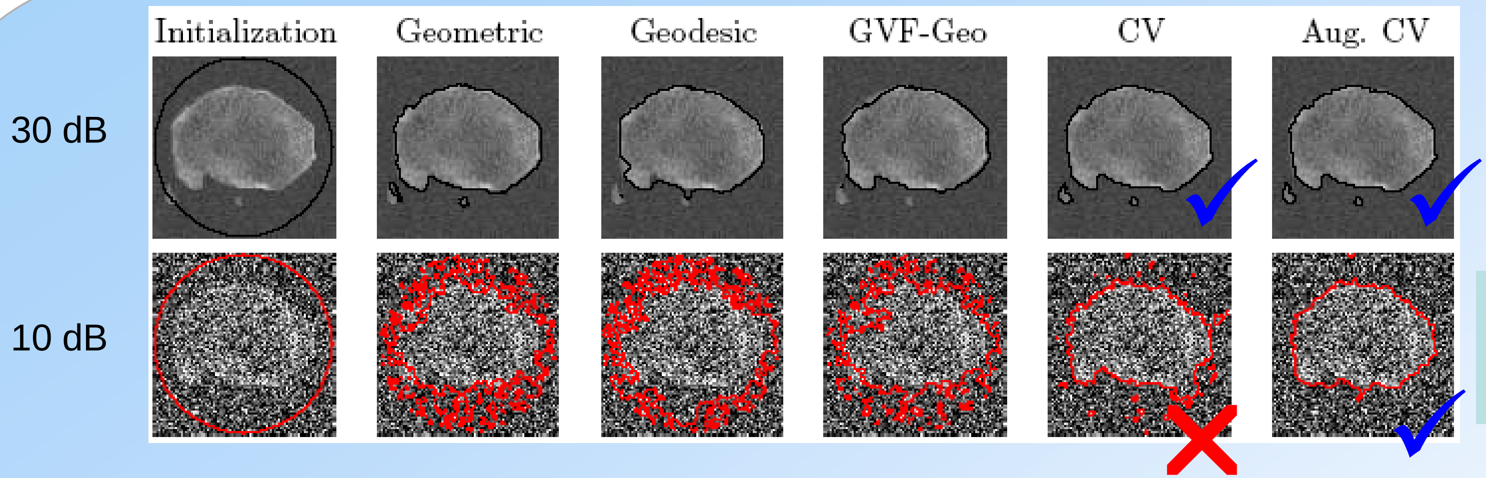

The proposed AC is least noise-sensitive.

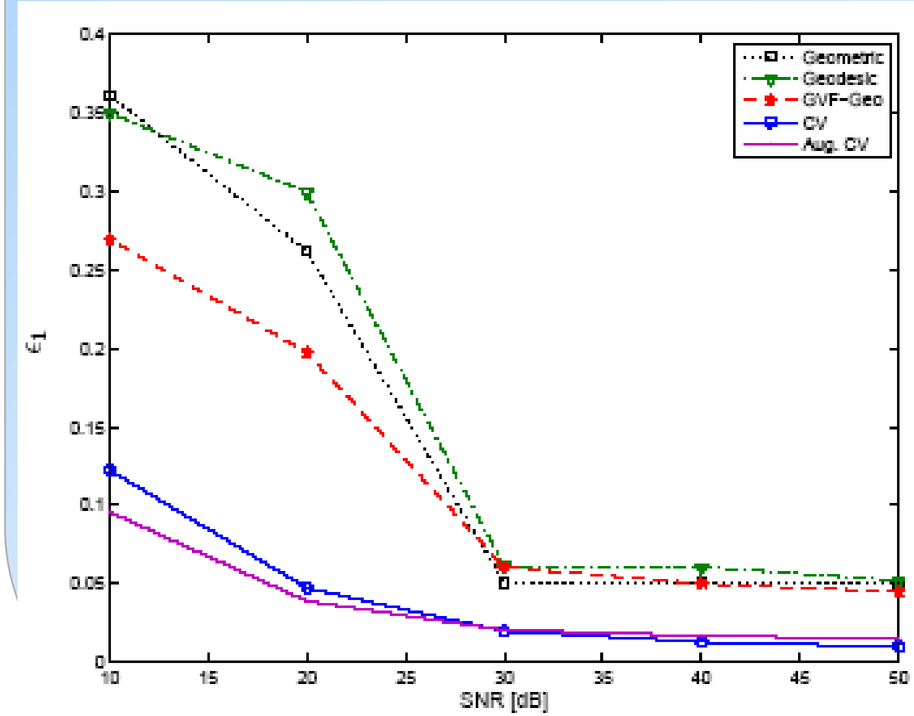

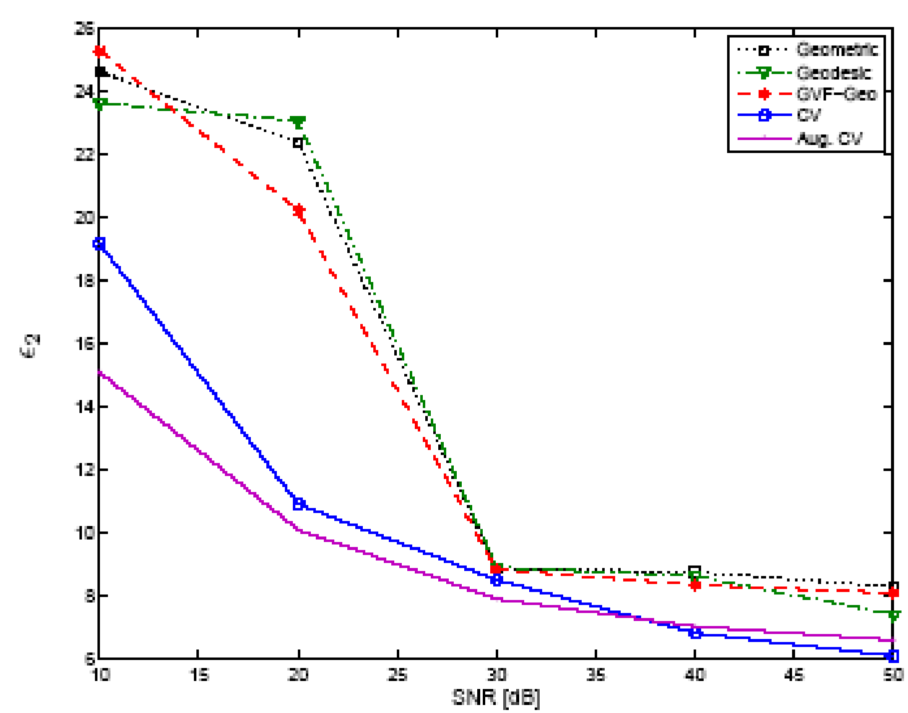

Contrast Sensitivity

Contrast
13 %

1%

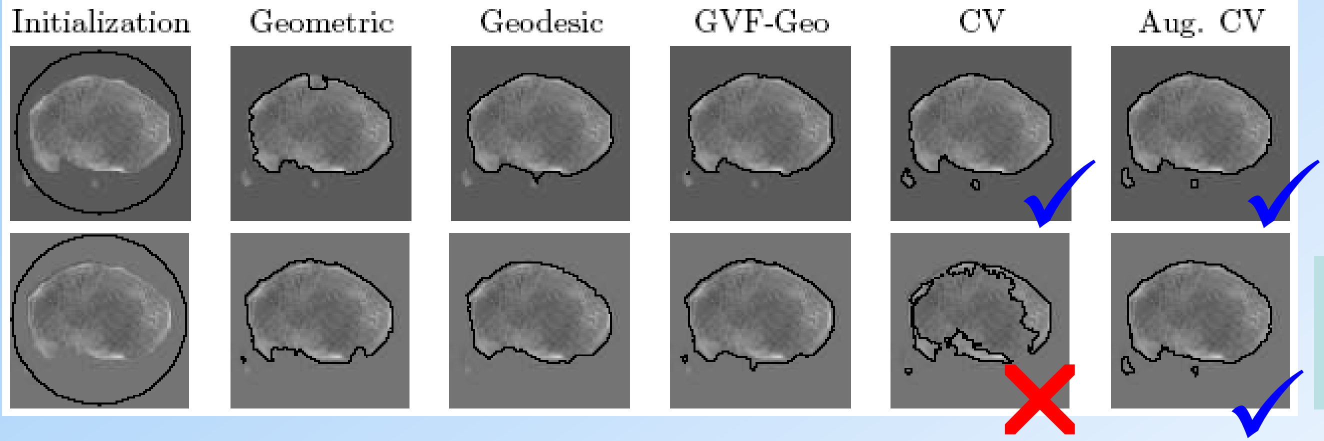

The CV AC is very contrast-sensitive.

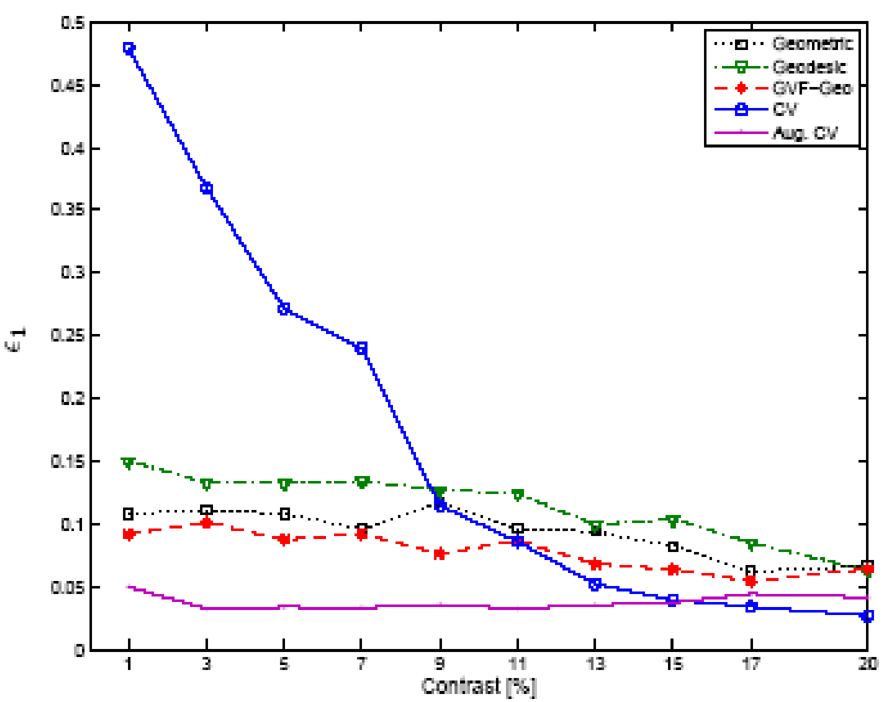

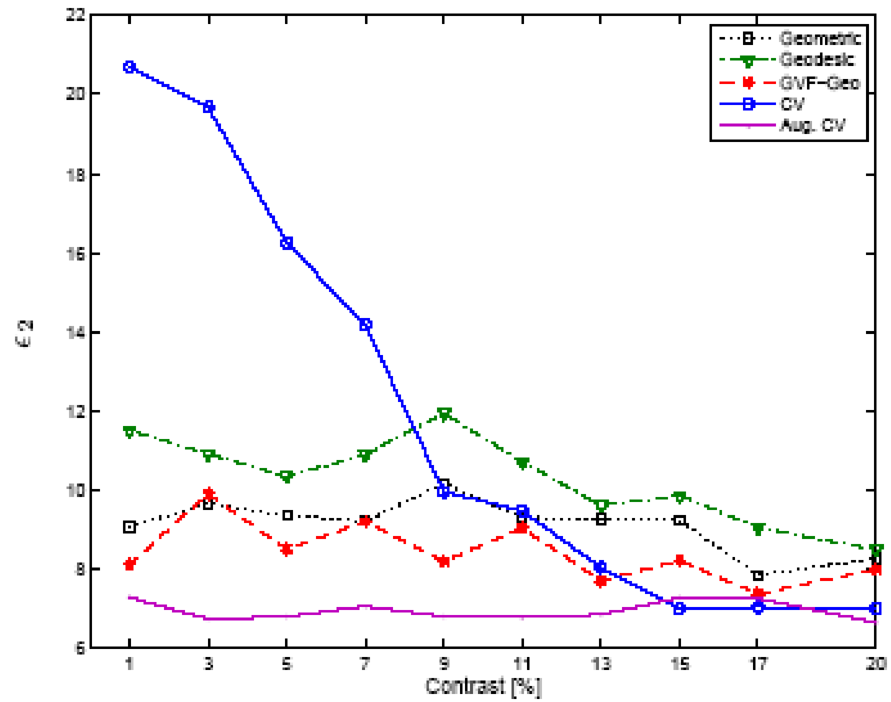

Real CT Images

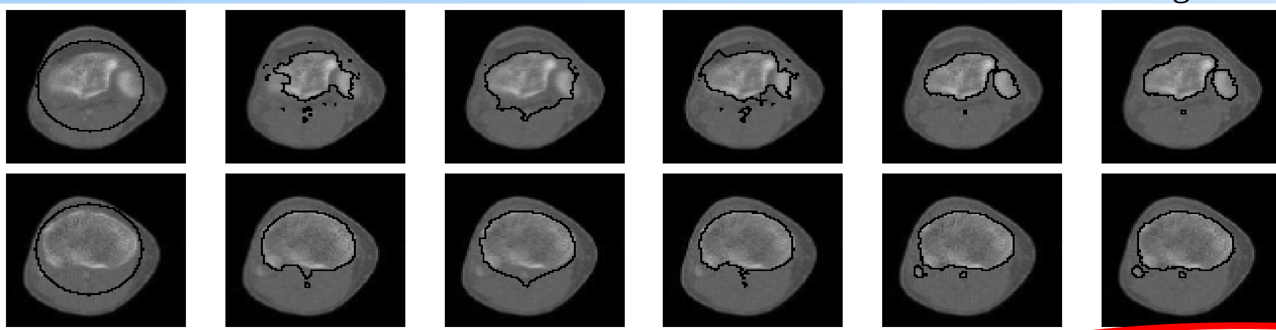

	Geome.	Geode.	GVF-Geo.	CV	Aug. CV	3D-DOCTOR
ϵ_1	0.184 (0.078)	0.155 (0.078)	0.147 (0.068)	0.086 (0.016)	0.089 (0.013)	0.078 (0.012)
ϵ_2	12.741 (3.240)	10.846 (3.924)	11.623 (3.313)	6.764 (1.542)	7.120 (1.537)	7.491 (1.490)

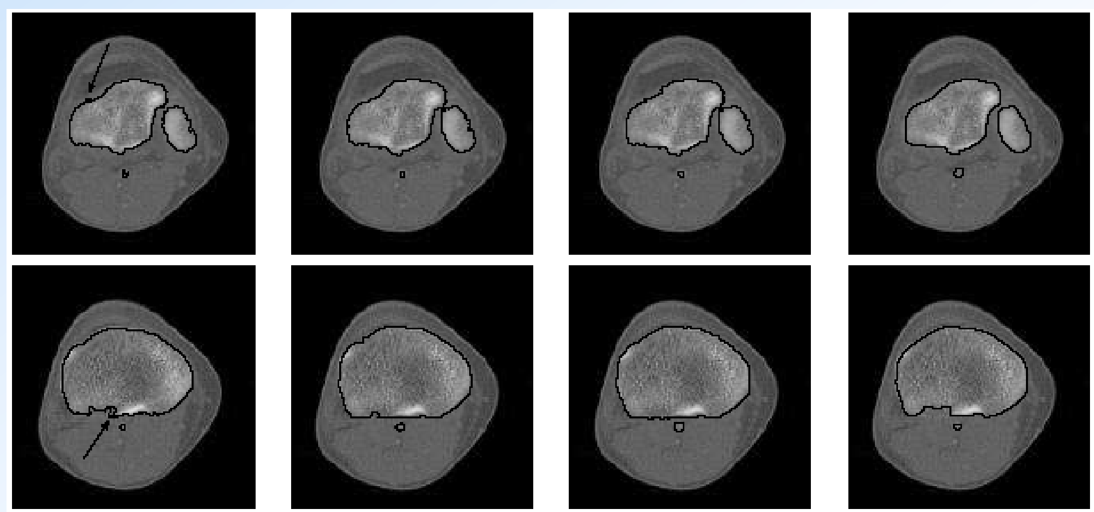

3D-DOCTOR:
a commercial software,
approved by FDA.

Sensitivity to β

Performances of Aug. CV AC applied on the real CT data set vs. β values

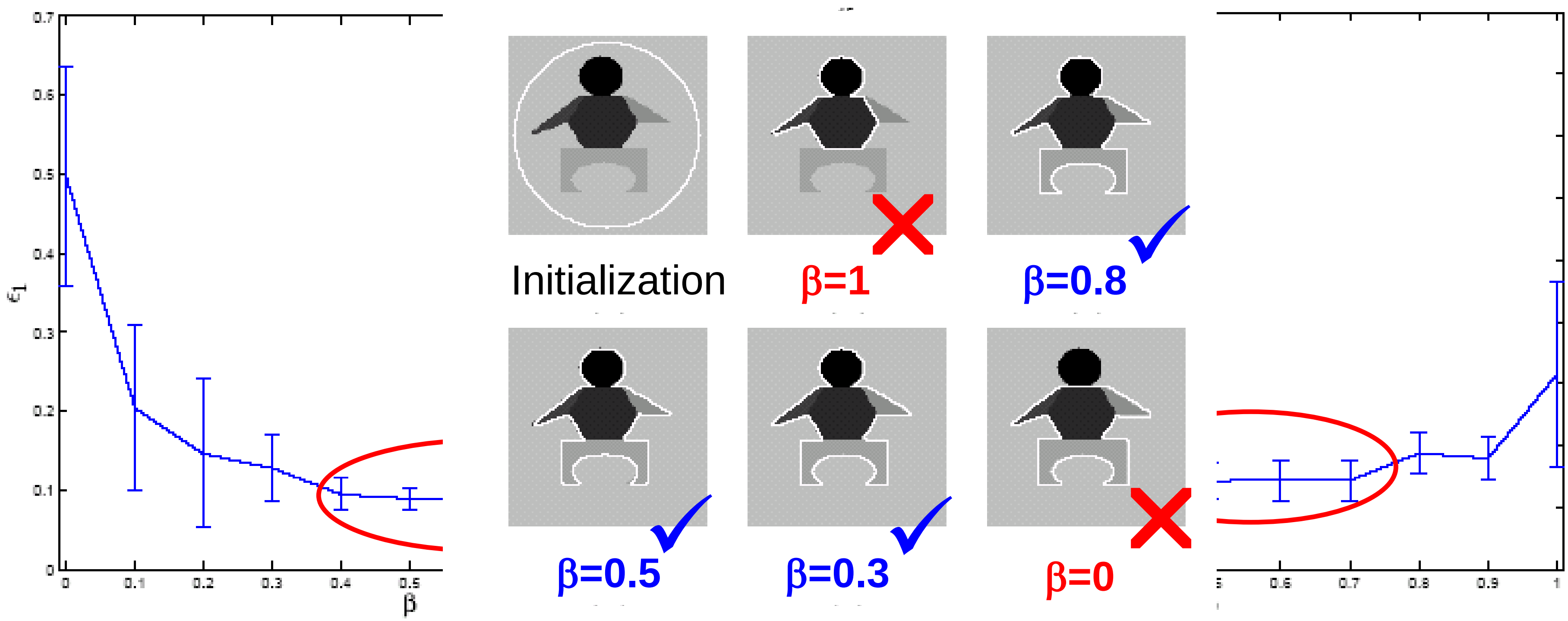

This model is not much β-sensitive since it performs well with many β values ranging from 0.4 to 0.7.

Discussions

- Aug. CV AC overcomes limitations of the classical CV AC when dealing with ***low contrast*** images and images having ***inhomogeneous objects***.
  - Less sensitive to noise.
  - Faster despite higher computational cost.
  - How to choose parameters systematically? – Unsolved.
- Quantitative evaluation on large data sets of medical images will be done in our future work to quantify its effectiveness in clinical usage.

Contributions

Technical

1. A novel approach for Hessian eigen-analysis with emphasis on preserving junctions while enhancing line structures
   - Calculating second-order derivatives in directional images
2. A new energy functional for segmenting inhomogeneous objects
   - Incorporating density distance into the Chan-Vese functional.

Medical

1. Vessel enhancement in angiography images
   - without junction suppression
   - more robust to noise
2. Automatic bone segmentation from CT images
   - topology adaptable
   - robust to noise and contrast

Publications

Patents

P-1. **P. T. H. Truc**, M. Khan, S. Y. Lee, and T.-S. Kim, “Vessel Enhancement using Decimation-free Directional Filter Bank”, US Patent (application number: 11/892,030).

Journals

J-1. **P. T. H. Truc**, M. Khan, Y.-K. Lee, S. Y. Lee, T.-S. Kim, “Vessel Enhancement Filter using Directional Filter Bank”, Comput. Vis. Image Understand. (SCI 1.5), in press, 2008 (doi:10.1016/j.cviu.2008.07.009).
J-2. **P. T. H. Truc**, T.-S. Kim, Y. H. Kim, Y.-K. Lee, and S. Y. Lee, “Automatic Bone Segmentation from CT Images using Chan-Vese Multiphase Active Contour”, Journal of Biomedical Engineering Research, vol. 28 (6), pp. 713-720, 2007.
J-3. M. Khan, **P. T. H. Truc**, R. Bahadur and S. Javed, “Vessel Enhancement using Directional Features”, Information Technology Journal 6 (6), pp. 851-857, 2007 (SCOPUS).
J-4. **P. T. H. Truc**, T.-S. Kim, Y.-K. Lee, S. Y. Lee, “A study on the feasibility of Active Contours on CT bone segmentation”, J. Digit. Imaging (SCI 0.7), under review.
J-5. **P. T. H. Truc**, T.-S. Kim, Y.-K. Lee, S. Y. Lee, “Homogeneity- and Density Distance-driven ACs in Medical Image Segmentation”, Phys. Med. Biol. (SCI 2.5), to be submitted.

Conferences

C-1. **P. T. H. Truc**, S. Y. Lee, and T.-S. Kim, “A Density Distance Augmented Chan-Vese Active Contour for CT Bone Segmentation”, 30th Annual Int. Conf. of IEEE in Medicine and Biology Society (IEEE EMBC’08), pp. 482-485, Vancouver, Canada, Aug. 2008.
C-2. **P. T. H. Truc**, M. Khan, S. Y. Lee, and T.-S. Kim, “Vessel Enhancement in Angiography Images using Decimation-free Directional Filter Bank”, IPCV'07, pp. 175-181, USA, Jun. 2007 (acceptance rate 28%).
C-3. **P. T. H. Truc**, M. Khan, S. Y. Lee, and T.-S. Kim, “A New Approach to Vessel Enhancement in Angiography Images”, IEEE/ICME Int. Conf. on Complex Medical Engineering, pp. 878-884, Beijing, China, May 2007.
C-4. **P. T. H. Truc**, Y. H. Kim, Y.-K. Lee, S. Y. Lee, and T.-S. Kim, “Evaluation of Active Contour-based Techniques toward Bone Segmentation from CT Images”, World Congress on Medical Physics and Biomedical Engineering, pp. 2997-3000, Seoul, Korea, 2006.
C-5. Nguyen Duc Thang, **P. T. H. Truc**, Young-Koo Lee, Sungyoung Lee, and Tae-Seong Kim, “3-D Human Pose Estimation from 2-D Depth Images”, Int. Conf. Ubiquitous Healthcare, Busan, Korea, Nov 2008.
C-6. A. M. Khan, **P. T. H. Truc**, Y. K. Lee, and T.-S. Kim, “A Tri-axial Accelerometer Sensor-based Human Activity Recognition via Augmented Signal Features and Hierarchical Recognizer”, Int. Conf. Ubiquitous Healthcare, Busan, Korea, Nov 2008.
C-7. J. J. Lee, Md. Zia Uddin, **P. T. H. Truc**, and T.-S. Kim, “Spatiotemporal Depth Information-based Human Facial Expression Recognition Using FICA and HMM”, Int. Conf. Ubiquitous Healthcare, Busan, Korea, Nov 2008.
C-8. Jehad Sarkar, **P.T.H. Truc**, Y.-K. Lee, and S.Y. Lee, “Statistical Language Modeling approach to Activity Recognition”, Int. Conf. Ubiquitous Healthcare, Busan, Korea, Nov 2008.
C-9. Md. Zia Uddin, J. J. Lee, **P. T. H. Truc**, and T.-S. Kim, “Human Activity Recognition Using Independent Component Features from Depth Images”, Int. Conf. Ubiquitous Healthcare, Busan, Korea, Nov 2008.

Acknowledgments

- Prof. S.Y. Lee and Y.-K. Lee
  - Excellent supervising and guidance
- Prof. T.-S. Kim and Prof. Md. A. U. Khan
  - Precious advices and discussions
- Prof. O.-S. Chae
  - Interesting DIP lectures
- Thesis defense committee
  - Invaluable comments
- Members of AR Team, Bio-Imaging Lab, and UC Lab
  - Collaboration and encouragement
- Family
  - Support and encouragement.